Thomas Jefferson University

Annual Progress Report: 2008 Formula Grant

Reporting Period

July 1, 2010 – June 30, 2011

Formula Grant Overview

The Thomas Jefferson University received $3,455,597 in formula funds for the grant award period January 1, 2009 through December 31, 2012. Accomplishments for the reporting period are described below.

Research Project 1: Project Title and Purpose

Role and Regulation of Focal Adhesion Kinase in Melanoma - Malignant melanoma is the deadliest form of skin cancer. Currently, the spreading of melanoma, known as metastasis, is only preventable by early detection and surgical excision of primary tumors. Therefore, it is critical that we understand the mechanisms underlying melanoma initiation and progression. The depth of invasion of a melanoma into the skin (dermis) is a determinant of treatment outcome. A gene, labeled B-RAF, is mutated in two-thirds of melanomas. This project has identified a target of the B-RAF gene known as focal adhesion kinase (FAK). This study will test whether B-RAF regulates FAK, which in turn promotes melanoma cell invasion into the dermis. Ultimately, the focus of this project is to identify why melanomas display invasive growth and, in doing so, identify novel targets for therapeutic intervention.

Anticipated Duration of Project

1/1/2009 - 12/31/2012

Project Overview

Malignant melanoma is the deadliest form of skin cancer and is poorly treatable. Depth of melanoma invasion into the dermis is used as a clinical determinant for prognosis. The long-term goal is to determine mechanisms underlying invasive growth of human melanomas. Mutations in the B-RAF gene are found in 50-70% of melanomas, and mutant B-RAF activation of the MEK-ERK1/2 pathway is required for invasion and resistance to apoptosis. Additionally, signaling from interaction with the surrounding extracellular matrix promotes invasion. Our preliminary data show that B-RAF-MEK-ERK1/2 signaling controls the phosphorylation of focal adhesion kinase (FAK) at serine 910. FAK localizes to sites of cell interaction with its extracellular matrix. Since these interactions regulate cell invasion, the goal of this project is to determine the role of serine 910 phosphorylation of FAK in melanoma cell invasion.

In Specific Aim 1, the hypothesis that phosphorylation of FAK at serine 910 regulates FAK

localization and turnover in focal adhesions, and cellular migration and invasion, will be tested. Experiments will utilize live cell imaging, cell migration and invasion assays. Analysis of cellular properties in complex multi-cell type systems is critical to mimic the *in vivo* situation. Thus, in Specific Aim 2, experiments will determine the requirement of FAK in invasive melanoma growth in a 3-D human skin reconstruct system. Further studies will test the role of serine 910 phosphorylation of FAK in this system. Overall, the study is designed to identify new mechanisms underlying B-RAF regulation of invasive properties in melanoma.

Principal Investigator

Andrew E. Aplin, PhD
Associate Professor
Thomas Jefferson University
Kimmel Cancer Center
5th Fl., Bluemle Bldg
233 South 10th Street
Philadelphia, PA 19107

Other Participating Researchers

Melanie Mayberry, MSc, Yongping Shao, PhD – employed by Thomas Jefferson University

Expected Research Outcomes and Benefits

At the completion of the project, we expect to have identified a protein that plays a critical role in melanoma cell invasion and understand what regulates its properties. This is a key question, since invasive melanoma is associated with a poor patient prognosis. Ultimately, this work could provide avenues to develop new therapeutic strategies for the treatment of melanoma. These avenues could be in combination with existing treatments, and may be particularly important in patients who develop resistance to initial treatments. Furthermore, a focus of this project is to discover a marker that will serve to identify particularly invasive, and thus aggressive, forms of melanoma.

Summary of Research Completed

Mutations within the serine kinase, BRAF, occur in approximately two-thirds of melanomas. The majority of mutations in BRAF lead to hyper-activation of the MEK-ERK1/2 pathway. *In vitro* and *in vivo* xenograft studies demonstrating a requirement for B-RAF in the proliferation, survival, and invasion of mutant BRAF melanoma cells have formed the pre-clinical basis for RAF inhibitors in clinical trials. Vemurafenib (PLX4032/RG7204), a selective inhibitor of mutant BRAF recently completed phase III randomized trials. PLX4032 elicited an objective response of 48%, compared to the 5% partial response seen with dacarbazine (standard of care). Furthermore, PLX402 progression-free survival was 5.3 months while 1.6 months of progression-free survival was observed with dacarbazine. Although PLX4032 has performed better than the standard of care treatment for metastatic melanoma, patients relapse and new

metastatic lesions are detected. In most instances relapse tumors have reactivation of the MEK-ERK1/2 pathway.

The goal of this project is to determine effects of mutant B-RAF-dependent phosphorylation of the focal adhesion kinase (FAK) in the malignant properties of melanoma cells. We have demonstrated in preliminary data that phosphorylation of FAK at serine 910 is dependent on active B-RAF signaling in human melanoma cells. In our continuing efforts to determine the role of serine phosphorylation in focal adhesion kinase (FAK) localization, we analyzed serine 910 phosphorylation in PLX-resistant mutant B-RAF melanoma cells. For these studies we utilized PLX4720, the pre-clinical analog of PLX4032. Chronic treatment with PLX4720 led to the emergence of cells (WM793-Res) resistant to PLX4720 induced cell cycle arrest (Figure 1A). Interestingly, these resistant cells displayed a characteristic morphology; they were more elongated than WM793 parental cells. Actin staining, with TRITC-phalloidin, revealed that resistant cells exhibit fewer cortical actin filaments compared to their parental counterparts (Figure 1B).

Immunoblotting with anti-FAK S910 antibody of WM793 parental and WM793-Res treated with PLX4720 for a 24 hour time course revealed that FAK phosphorylation at S910 was unaffected by PLX4720 treatment throughout the entire time course (Figure 2, left panel). However, treatment of WM793 parental cells with PLX4720 led to a decrease in FAK phosphorylation at S910 within 4 hours (Figure 2, right panel).

These findings prompted us to analyze the effects of PLX4720 further upstream in the pathway. Consistent with prior reports, PLX4720, effectively blocked MEK and ERK1/2 activation in the mutant B-RAF harboring vertical growth cell line, WM793 (Figure 2, left panel). By contrast, treatment of WM793-Res with PLX4720 did not inhibit MEK and ERK1/2 activation (Figure 2, right panel).

Publications arising from this work:

Kaplan, F., Shao, Y., Mayberry, M. and Aplin, A.E. (2011) Hyperactivation of MEK-ERK1/2 signaling and resistance to apoptosis induced by PLX4720 in mutant N-RAS melanoma cells. Oncogene 30:366-71. Epub 2010 Sep 6.

Aplin, AE, Kaplan, FM and Shao, Y. Mechanisms of resistance to B-RAF inhibitors in melanoma. J Invest Dermatol advance online publication, May 19, 2011; doi:10.1038/jid.2011.147

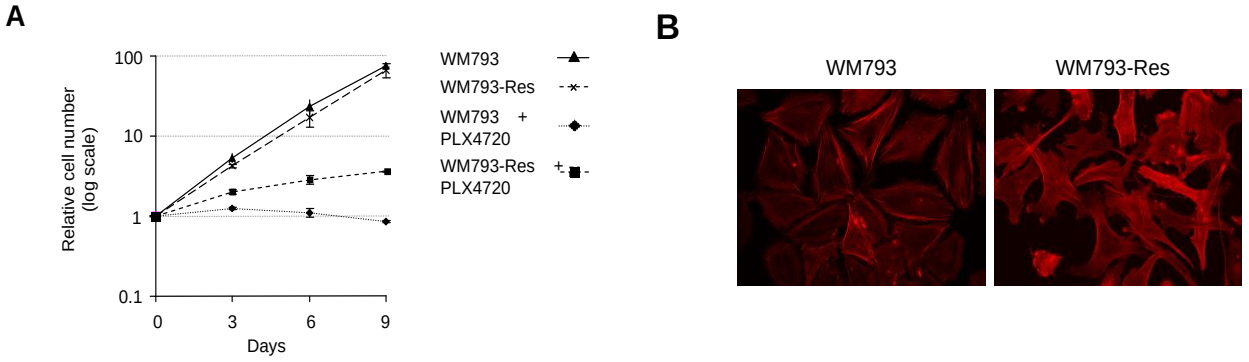

Figure 1. WM793-Res cells have altered growth and cell morphology. (A) Parental and resistant WM793 (WM793-Res) cells were grown in media -/+ 5 µM PLX4720 for 9 days. Drugs were replenished every 48 hours. Cells were counted every 3 days, normalized against starting number and plotted for each time points indicated. X axis, time points; Y axis, mean relative cell number from triplet experiments. Error bars = standard deviations. (B) TRITC-phalloidin staining of parental and resistant WM793 cells.

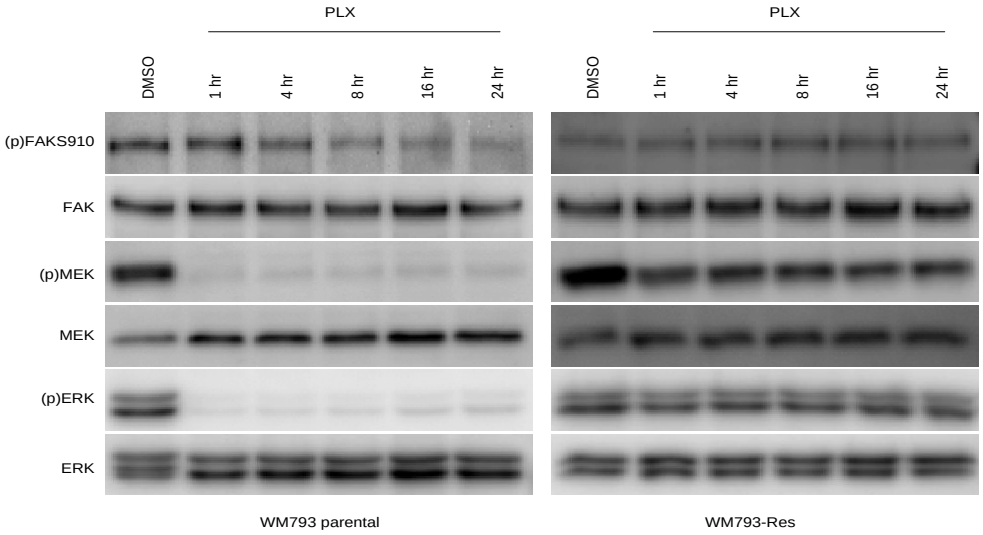

Figure 2. WM793-Res cells have stable ERK1/2 activity in the presence of PLX4720. WM793 parental and WM793-Res cell lines were treated with DMSO and 1 µM PLX4720 (PLX) [Plexxikon] for up to 24 hours. Western blot analysis was performed on MEK-ERK1/2 pathway proteins and FAK, as indicated. ERK was used as a loading control.

Research Project 2: Project Title and Purpose

Prolactin and Growth Factor Signaling in Breast Cancer - Progression of breast cancer from early solitary lesions to advanced metastatic disease requires loss of cellular differentiation and epithelial-to-mesenchymal transition (EMT). While extensive efforts have been devoted to understanding the factors that allow this transition to occur in breast cancer, little work has focused on factors that prevent EMT, or on molecular strategies to reverse EMT for use in

differentiation therapy. The long-range goal of this laboratory is to identify molecular mechanisms that govern growth and cellular differentiation of human breast cancer to improve therapies, and to use this knowledge to improve drug responsiveness of individual tumors, so that more effective, personalized medical treatment can be realized for cancer patients.

Anticipated Duration of Project

1/1/2009 - 12/31/2012

Project Overview

The central hypothesis is that the prolactin receptor (PRLR)-Jak2-Stat5 pathway in breast cancer is inhibited by growth factor receptor signaling, which in turn promotes loss of estrogen receptor (ER) expression and epithelial-to-mesenchymal transition (EMT).

Aim #1 Determine whether the PRLR-Jak2-Stat5 pathway in human breast cancer is inhibited by EMT-promoting growth factors in the tumor microenvironment. The hypothesis is that paracrine growth factor receptor activation by epidermal growth factor (EGF) ligands inhibits the differentiation-promoting PRL-Jak2-Stat5 pathway in breast cancer, through a mechanism that involves Erk1/2 phosphorylation of Jak2 on the inhibitory Ser523 residue. We will *a)* determine whether experimental EGFR/Her2-mediated signaling inactivates PRL-induced Stat5 activation in breast cancer lines through Jak2 inhibition, due to activation of either Erk1/2, Jnk and/or Akt pathways, and *b)* analyze whether signaling by EGF receptors and hyperactivation of Erk1/2, Jnk and/or Akt kinases is associated with inactivation of Stat5 in two large sets of human breast cancer specimens (n=850).

Aim #2 Determine whether Stat5a activation is sufficient to overcome dedifferentiation, EMT, and loss of ERα induced by EGFR/Her2 in human breast cancer. The hypothesis is that EGFR/Her2 inhibition of the PRLR-Jak2-Stat5 pathway is required for EGFR/Her2-induced EMT, cell-cycle progression, and loss of ERα expression. We will determine *a)* whether Stat5 reactivation overcomes EGFR/Her2-induced EMT, and *b)* whether Stat5 reactivation restores ERα expression in ERα-negative, EGFR/Her2-positive breast cancer *in vitro* and *in vivo*.

Principal Investigator

Hallgeir Rui, MD, PhD
Professor
Thomas Jefferson University
Kimmel Cancer Center
10th Fl., Bluemle Bldg
233 South 10th Street
Philadelphia, PA 19107

Other Participating Researchers

Fransiscus Utama, PhD – employed by Thomas Jefferson University

Expected Research Outcomes and Benefits

More than one million new cases of breast cancer are diagnosed each year worldwide, and an estimated 370,000 women die each year. The majority of breast cancer fatalities are caused by metastasis (spreading to other organs) of the primary tumor. Identifying the molecular changes that lead to metastatic progression is critical for developing better strategies to prevent spreading and treat advanced breast cancer. While it is generally accepted that loss of differentiation and epithelial-to-mesenchymal transition (EMT) are required for breast cancer metastasis, efforts to reverse de-differentiation of breast cancer have been limited.

The Stat5 protein is a suppressor of human breast cancer dedifferentiation, invasion, and progression. Studies are also designed to determine whether pharmacologic inhibition of EGFR/ErbB2 will restore prolactin (PRL)-Jak2-Stat5a/b signaling in breast cancer *in vitro* and *in vivo*. This is important because PRL is a key activator of Stat5 in normal and malignant breast epithelia. If our hypotheses are correct, EGFR/Her2 inhibition combined with Stat5 hyperactivation (e.g., by prolactin or Stat5-ptpase inhibitors) plus antiestrogens may be effective against aggressive ERα-negative, EGFR/Her-2 positive breast cancer.

Furthermore, combined biomarker analyses of Stat5, ERα and EGFR/Her-2 are expected to improve diagnostic classification of human breast cancer and prediction of response to targeted therapies. More effective personalized medicine for breast cancer patients could be a result. Finally, the scientific environment at the Kimmel Cancer Center at Thomas Jefferson University is highly collaborative and the possibilities for translational research are outstanding, so that if successful, the project can move forward with clinical trials.

Summary of Research Completed

Novel Progress related to Aim 1 showing that activation of transcription fact Stat3 correlated with Stat5 activation in breast cancer but did not have prognostic value.

Research related to Aim 1 completed during this reporting period has resulted in novel discoveries. Signal transducer and activator of transcription-3 (Stat3) is frequently activated in breast cancer and multiple lines of evidence suggest that Stat3 promotes tumor progression. However, the prognostic value of Stat3 in human breast cancer remains controversial and associations range from favorable to unfavorable based on four published outcome studies of 62, 102, 255 and 517 patients. Cellular Stat3 protein expression was measured in three of the published studies whereas nuclear localized, tyrosine phosphorylated Stat3 (Nuc-pYStat3) was used as the readout in only one of the published studies. We therefore retrospectively analyzed the prognostic value of Nuc-pYStat3 in a larger material of 721 breast cancer specimens.

Overall, patients whose tumors were positive for Nuc-pYStat3 tended to have improved survival, but the trend did not reach statistical significance (P=0.08). When specimens were stratified by tumor grade, patients with low grade, but not high grade tumors, that were positive for Nuc-pYStat3 had significantly prolonged overall survival in univariate analysis (P=0.014), but not in multivariate analyses. Unexpectedly, quantitative immunofluoresence detection revealed highest levels of Nuc-pYStat3 in normal breast epithelia and gradual loss of Nuc-pYStat3 during

progression from DCIS, invasive ductal carcinoma, and lymph node metastases. Levels of Nuc-pYStat3 correlated positively with levels of Nuc-pYStat5, a favorable prognostic marker, in invasive ductal carcinomas. Furthermore, Nuc-pYStat3 levels correlated strongly with protein levels of nuclear localized Stat5a ($r=0.633$, $P<0.001$), but not Stat5b. Our data does not support the notion that Nuc-pYStat3 is an independent marker of prognosis in breast cancer, although future studies may reveal prognostic utility of Nuc-pYStat3 within molecularly characterized subtypes of breast cancer.

Novel progress that relates to Aim 2 is data showing that Stat5a status predicts prognosis and response to anti-estrogen therapy.

Purpose: Nuclear-localized and tyrosine-phosphorylated Stat5a/b has been reported as a favorable prognostic marker and predictor of response to antiestrogen therapy. However phospho-antibodies do not distinguish Stat5a from closely related Stat5b. The purpose of this study was to determine if levels of nuclear localized Stat5a protein (Nuc-Stat5a), the most prevalent Stat5 protein in the breast, was a more appropriate marker of survival and antiestrogen response.

Experimental Design: Stat5a was detected by traditional diaminobenzidine-chromogen immunohistochemistry or by immunofluorescence in five archival cohorts of breast cancer. Nuclear localization of Stat5a was evaluated by pathologist scoring of whole tissue sections detected by immunohistochemistry or automated quantitative analysis (AQUA) of immunofluorescently-labeled tissue microarrays. Breast cancer-specific survival (CSS) and time to recurrence (TTR) were analyzed according to Nuc-Stat5a status using univariate and multivariate statistical models, adjusting for clinical features including tumor grade, size, lymph node and hormone receptor status.

Results: Levels of Nuc-Stat5a were reduced in invasive breast cancer tissues and lymph node metastases compared to normal tissue and ductal carcinoma *in situ* (Material I; n=180). Node negative breast cancer patients with low expression of nuclear Stat5a, detected by standard IHC (Material II; n=223) or quantitative analysis (Material III; n=198), had poor breast cancer outcome as measured by univariate and multivariate CSS (Material II/III) and TTR (Material II). CSS and TTR analysis of two independent materials analyzed by standard IHC (Material IV; n=73) or quantitative immunofluorescence (Material V; n=97) indicated that antiestrogen-treated patients whose tumors expressed low levels of Nuc-Stat5a were at a greater than 4-fold risk of antiestrogen therapy failure when adjusted for clinical features (multivariate CSS: Material IV HR=4.3 (1.2,15.6), $p=0.03$; Material V HR=5.0 (1.87,13.06), $p=0.001$).

Conclusions: Loss of Nuc-Stat5a is a promising independent marker of poor breast cancer prognosis in node-negative, non-adjuvant treated breast cancer patients. Additionally, Nuc-Stat5a may be a useful clinical tool to predict tumor response to antiestrogen therapy.

Table 1. Characteristics of Cohort I, II, IV, and V. ER - estrogen receptor; PR - progesterone receptor; SD - standard deviation.

Discrete Variables		Cohort I (N = 233) Number (%)	Cohort II (N = 291) Number (%)	Cohort IV (N = 221) Number (%)	Cohort V (N = 97) Number (%)
Center	Fox Chase Cancer Center	64 (27)	--	--	--
	Kaiser Permanente	79 (34)	--	--	--
	University of Miami	30 (13)	--	--	--
	Washington University	60 (26)	--	--	--
	Basel	--	--	221 (100)	--
Race	Asian	1 (0.4)	--	0 (0)	--
	Black	16 (7)	3 (1)	0 (0)	--
	White	216 (93)	287 (99)	0 (0)	--
	Other	--	1 (0.3)	0 (0)	--
	Unknown	--	--	221 (100)	--
Age	<50 yrs	42 (18)	86 (30)	27 (12)	6 (6)
	≥50 yrs	191 (82)	205 (70)	194 (88)	91 (94)
Tumor Size	<2cm	117 (50)	114 (39)	53 (24)	39 (40)
	≥2cm, <5cm	107 (46)	133 (46)	142 (64)	43 (44)
	≥5cm	9 (4)	33 (11)	23 (10)	11 (11)
	Missing	--	11 (4)	3 (1)	4 (4)
Grade	1	61 (26)	67 (23)	56 (25)	14 (14)
	2	104 (45)	137 (47)	99 (45)	47 (48)
	3	68 (29)	48 (16)	66 (30)	32 (33)
	Missing	--	39 (13)	--	4 (4)
ER Status	Negative	44 (19)	97 (33)	44 (20)	11 (11)
	Positive	186 (80)	163 (56	130 (59)	80 (82)
	Missing	3 (1)	31 (11)	47 (21)	6 (6)
PR Status	Negative	65 (28)	103 (35)	87 (39)	25 (26)
	Positive	122 (52)	151 (52)	134 (61)	67 (69)
	Missing	46 (20)	37 (13)	--	5 (5)
Her2 Status	Non-overexpressed	--	217 (75)	173 (78)	77 (79)
	Over-expressed	--	33 (11)	29 (13)	13 (13)
	Missing	--	41 (14)	19 (9)	7 (7)
Node Status	Negative	233 (100)	291 (100)	70 (32)	42 (43)
	Positive	0 (0)	0 (0)	138 (62)	42 (43)
	Missing	--	--	13 (6)	13 (13)
Chemotherapy	Untreated	233 (100)	--	171 (77)	95 (98)
	Treated	0 (0)	--	45 (20)	1 (1) †
	Missing	--	--	5 (2)	1 (1)
Hormone Therapy	Untreated	233 (100)	--	0 (0)	5 (5)
	Treated	0 (0)	--	221 (100)	92 (95)
Radiation Therapy	Untreated	187 (80)	--	221 (100)	36 (37)
	Treated	46 (20)	--	0 (0)	59 (61)
	Missing	--	--	--	2 (2)
CSS Events		52 (22)	107 (37)	65 (29)	56 (58)
Nuc-pYStat5 Status	Low	129 (55)	84 (29)	93 (42)	10 (10)
	High	94 (40)	114 (39)	73 (33)	55 (57)
	Missing	10 (4)	93 (32)	55 (25)	32 (33)
Continuous Variables		**Mean**	**Median**	**Range**	**SD**
Cohort I	Age at Diagnosis	62.3	62	31 - 88	12.9
	Tumor Size (cm)	2.08	1.8	0.6 - 7.5	1.07
	Followup (months)	129	126	3 - 326	71
	Nuc-pYStat5 score	5.0	0	0 - 40	8.6
	Year of Diagnosis	--	--	1974 - 1990	--
Cohort II	Age at Diagnosis	57.3	57	24 - 86	12.3
	Tumor Size (cm)	2.53	2.0	0.4 - 11	1.67
	Followup (months)	165	160	1 - 425	106
	Nuc-pYStat5 score	852	771	265 - 2236	416
	Year of Diagnosis	--	--	1953 - 1980	--

Cohort IV	Age at Diagnosis	63.3	63	35 - 97	12.1
	Tumor Size (cm)	3.0	2.5	0.5 - 13.0	1.8
	Followup (months)	59.0	60	2 - 137	28.0
	Nuc-pYStat5 score	1	0	0 - 4	1.3
	Positive Nodes	3.8	1	0 - 38	6.2
	Year of Diagnosis	--	--	1985 - 1996	--
Cohort V	Age at Diagnosis	69.8	72	38 - 89	11.0
	Tumor Size (cm)	2.7	2.1	0.4 - 11	1.7
	Followup (months)	57.5	40.7	3.6 - 143	40.9
	Nuc-pYStat5 score	1262	1027	533 - 4243	762
	Positive Nodes	2.3	0	0 - 22	3.7
	Year of Diagnosis	--	--	1990 - 2000	--

† Patient received chemotherapy following disease relapse.

Table 2. Univariate and multivariate survival analyses of breast cancer specific survival (CSS) in Cohort I and II. Weibull regression survival analysis was used to evaluate prognostic factors. HR - hazard ratio; CI - confidence interval; ER - estrogen receptor; PR - progesterone receptor.

Cohort I (CSS) **N = 233** **183 (79%) evaluable** **41/183 (22%) events**			**Multivariate Adjusted (Weibull)**†		**Unadjusted (Weibull)**	
Variable		**n**	**HR (95% CI)**	**p**	**HR (95% CI)**	**p**
Tumor Grade	1	47	1	---	1	---
	2	76	1.53 (0.57-4.10)	0.399	1.87 (0.72-4.87)	0.198
	3	60	1.61 (0.56-4.66)	0.381	2.74 (1.057.11)	0.039
Tumor Size	< 2cm	88	1	---	1	---
	≥ 2cm, < 5cm	87	2.30 (1.06-4.99)	0.036	2.47 (1.20-5.08)	0.014
	≥ 5cm	8	2.50 (0.62-10.04)	0.197	2.97 (0.80-10.95)	0.103
ER Status	Negative	32	1	---	1	---
	Positive	151	1.82 (0.70-4.71)	0.216	0.72 (0.34-1.51)	0.380
PR Status	Negative	64	1	---	1	---
	Positive	119	0.55 (0.25-1.20)	0.133	0.55 (0.29-1.04)	0.065
Nuc-pYStat5	Low (0)	105	2.38 (1.13-5.04)	0.023	2.32 (1.10-4.89)	0.027
	High (>0)	78	1	---	1	---
Cohort II (CSS) **N = 291** **158 (54%) evaluable** **61/158 (39%) events**			**Multivariate Adjusted (Weibull)**‡		**Unadjusted (Weibull)**	
Variable		**n**	**HR (95% CI)**		**HR (95% CI)**	**p**
Tumor Grade	1	34	1	---	1	----
	2	90	1.25 (0.66-2.37)	0.500	1.16 (0.62-2.19)	0.640
	3	34	0.87 (0.35-2.19)	0.772	0.81 (0.36-1.82)	0.616
Tumor Size	< 2cm	60	1	----	1	----
	≥ 2cm, < 5cm	80	2.49 (1.33-4.67)	0.004	2.11 (1.15-3.88)	0.016
	≥ 5cm	18	3.89 (1.63-9.26)	0.002	2.68 (1.19-6.05)	0.018
ER Status	Negative	50	1	----	1	----
	Positive	108	0.88 (0.45-1.70)	0.698	1.01 (0.59-1.73)	0.958
PR Status	Negative	57	1	----	1	----
	Positive	101	1.26 (0.69-2.29)	0.459	0.92 (0.55-1.55)	0.757
Her2 Status	Negative	138	1	----	1	----
	Over-expressed	20	1.37 (0.61-3.07)	0.440	1.04 (0.49-2.19)	0.918
Nuc-pYStat5	Low (<684)	67	2.39 (1.37-4.17)	0.002	2.10 (1.26-3.51)	0.004
	High (≥684)	91	1	----	1	----

†/‡Global test for Cox regression proportional hazards assumption failed, necessitating Weibull regression
†Global test: $\chi^2(5) = 12.93$, $p = 0.024$
‡Global test: $\chi^2(6) = 13.22$, $p = 0.040$

Table 3. Univariate and multivariate breast cancer-specific survival (CSS) and time to recurrence (TTR) analysis of Nuc-pYStat5 in breast cancer patients treated with antiestrogen monotherapy in Cohort V. Cox regression survival analysis was used to evaluate prognostic factors. HR - hazard ratio; CI - confidence interval; ER/PR status - estrogen or progesterone receptor positive.

Cohort V (CSS) **N = 97** **53 (55%) evaluable** **31/53 (58%) events**			**Multivariate Adjusted (Cox)†**		**Unadjusted (Cox)**	
Variable		**n**	**HR (95% CI)**	**p**	**HR (95% CI)**	**p**
Tumor Size	< 2cm	25	1	---	1	---
	2 - <5cm	23	1.24 (0.42-3.66)	0.700	2.92 (1.33-6.41)	0.008
	≥ 5cm	5	0.97 (0.21-4.41)	0.971	4.83 (1.50-15.57)	0.008
Tumor Grade	1	8	1	---	1	---
	2	27	0.60 (0.19-1.88)	0.376	0.80 (0.29-2.26)	0.677
	3	18	0.73 (0.21-2.55)	0.621	1.64 (0.58-4.61)	0.347
ER/PR Status	Negative	8	1	---	1	---
	Positive	45	0.10 (0.03-0.39)	0.001	0.37 (0.16-0.88)	0.024
Her2 Status	Normal	45	1	---	1	---
	Over-expressed	8	1.99 (0.71-5.64)	0.193	2.53 (1.08-5.93)	0.032
Lymph Node Status	Negative	28	1	---	1	---
	Positive	25	8.10 (3.03-21.64)	<0.001	4.72 (2.19-10.20)	<0.001
Nuc-pYStat5	Low (<724)	8	21.55 (5.61-82.77)	<0.001	7.36 (2.94-18.42)	<0.001
	High (≥724)	45	1	---	1	---
Cohort V (TTR) **N = 97** **53 (55%) evaluable** **34/53 (64%) events**			**Multivariate Adjusted (Cox)‡**		**Unadjusted (Cox)**	
Variable		**n**	**HR (95% CI)**	**p**	**HR (95% CI)**	**p**
Tumor Size	< 2cm	25	1	---	1	---
	2 - <5cm	23	1.56 (0.56-4.35)	0.393	2.68 (1.27-5.68)	0.010
	≥ 5cm	5	1.81 (0.46-7.21)	0.397	5.28 (1.82-15.33)	0.002
Tumor Grade	1	8	1	---	1	---
	2	27	0.46 (0.16-1.35)	0.156	0.67 (0.26-1.75)	0.417
	3	18	0.70 (0.22-2.26)	0.553	1.53 (0.59-4.00)	0.384
ER/PR Status	Negative	8	1	---	1	---
	Positive	45	0.16 (0.05-0.49)	0.001	0.31 (0.14-0.71)	0.005
Her2 Status	Normal	45	1	---	1	---
	Over-expressed	8	2.02 (0.74-5.50)	0.171	2.33 (1.01-5.38)	0.048
Lymph Node Status	Negative	28	1	---	1	---
	Positive	25	5.28 (2.28-12.18)	<0.001	3.65 (1.80-7.42)	<0.001
Nuc-pYStat5	Low (<724)	8	7.30 (2.34-22.78)	0.001	4.71 (1.99-11.16)	<0.001
	High (≥724)	45	1	---	1	---

†/‡Global test for Cox regression proportional hazards passed
† Global test: $\chi^2(6) = 6.38$, $p = 0.38$
‡ Global test: $\chi^2(6) = 5.45$, $p = 0.49$

Supplementary Table 1. Univariate and multivariate Cox regression survival analyses of time to recurrence (TTR) of breast cancer in Cohort I. HR - hazard ratio; CI - confidence interval; ER - estrogen receptor; PR - progesterone receptor.

Cohort I* (TTR) **N = 233** **183 (79%) evaluable** **45/183 (25%) events**			**Multivariate Adjusted (Cox)†**		**Unadjusted (Cox)**	
Variable		**n**	**HR (95% CI)**	**p**	**HR (95% CI)**	**p**
Tumor Grade	1	47	1	---	1	---
	2	76	2.01 (0.77-5.25)	0.156	2.24 (0.89-5.67)	0.087
	3	60	2.05 (0.73-5.77)	0.174	3.41 (1.32-8.84)	0.012
Tumor Size	< 2cm	88	1	---	1	---
	≥ 2cm, < 5cm	87	2.13 (1.04-4.35)	0.038	2.41 (1.25-4.65)	0.009
	≥ 5cm	8	2.54 (0.67-9.57)	0.169	3.20 (0.90-11.34)	0.072
ER Status*	Negative	32			1	---
	Positive	151			0.83 (0.40-1.73)	0.622
PR Status	Negative	64	1	---	1	---
	Positive	119	0.36 (0.18-0.72)	0.004	0.35 (0.18-0.69)	0.002
Nuc-pYStat5	Low (0)	105	2.49 (1.23-5.05)	0.012	2.35 (1.18-4.67)	0.015
	High (>0)	78	1	---	1	---

†Global test for Cox regression proportional hazards passed; Global test: $\chi^2(4) = 3.84$, $p = 0.43$
*Stratified by ER Status, except for univariate (unadjusted) ER status which was done as Weibull

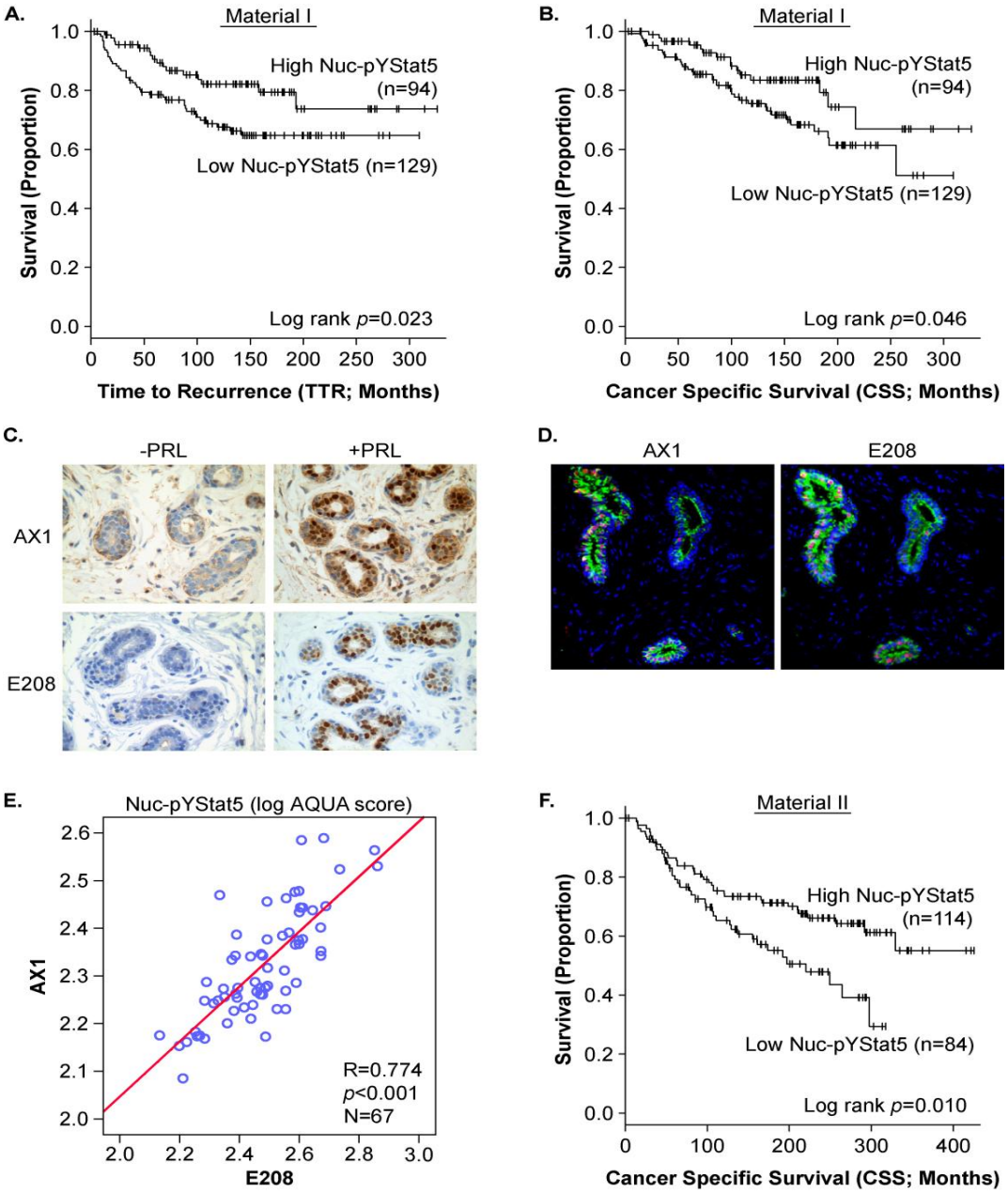

Figure 1. Low levels of Nuc-pYStat5 predict unfavorable breast cancer prognosis. (A-B) Kaplan-Meier analysis of Nuc-pYStat5, detected by mouse monoclonal anti-pYStat5 AX1 antibody and standard DAB IHC with pathologist review of whole tissue sections, in Cohort I revealed that low expression of Nuc-pYStat5 was prognostic of (A) reduced time to recurrence (TTR) of breast cancer and (B) poor breast cancer-specific survival (CSS). (C-E) Comparative validation of mouse monoclonal AX1 with rabbit monoclonal anti-pYStat5 antibody E208. (C) Detection of nuclear localized and tyrosine phosphorylated Stat5 by DAB-chromogen IHC in healthy human breast tissue surgical explants incubated *ex vivo* with (positive control) or without (negative control) human prolactin (100nM; 60min) using anti-pYStat5 antibodies AX1 (16 h incubation with manual staining protocol; upper panels) or E208 (20 min incubation with autostainer protocol; lower panels). (D) Representative immunofluorescent images from two serial sections of a breast tissue array stained with AX1 or E208 antibodies indicating comparable detection of Nuc-pYStat5. (E) Correlation of Nuc-pYStat5 expression detected by AX1 or E208 and quantified by AQUA in serial sections of an assorted breast tissue microarray. (F) Kaplan-Meier analysis of breast cancer-specific survival (CSS) in Cohort II indicated that risk of death from breast cancer was significantly elevated in patients whose tumors expressed low Nuc-pYStat5 as quantified by immunofluorescence and AQUA analysis. Censored cases (+) and number of patients per group are indicated.

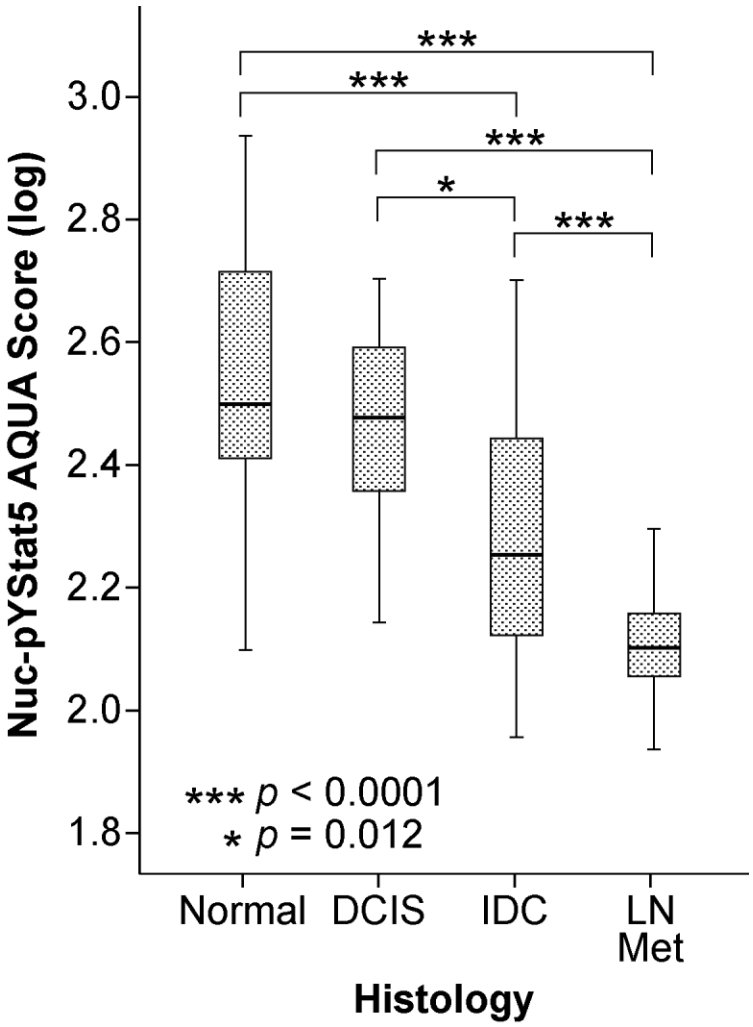

Figure 2. Loss of Nuc-pYStat5 during breast cancer progression. Levels of Nuc-pYStat5 as detected by immunofluorescence and quantified by AQUA were significantly reduced in invasive ductal carcinoma (IDC; n=72) and lymph node metastases (n=17) when compared to normal breast tissue (n=27) and ductal carcinoma *in situ* (DCIS; n=14) in progression array Cohort III. DCIS - ductal carcinoma *in situ*; IDC - invasive ductal carcinoma; LN Met - lymph node metastasis.

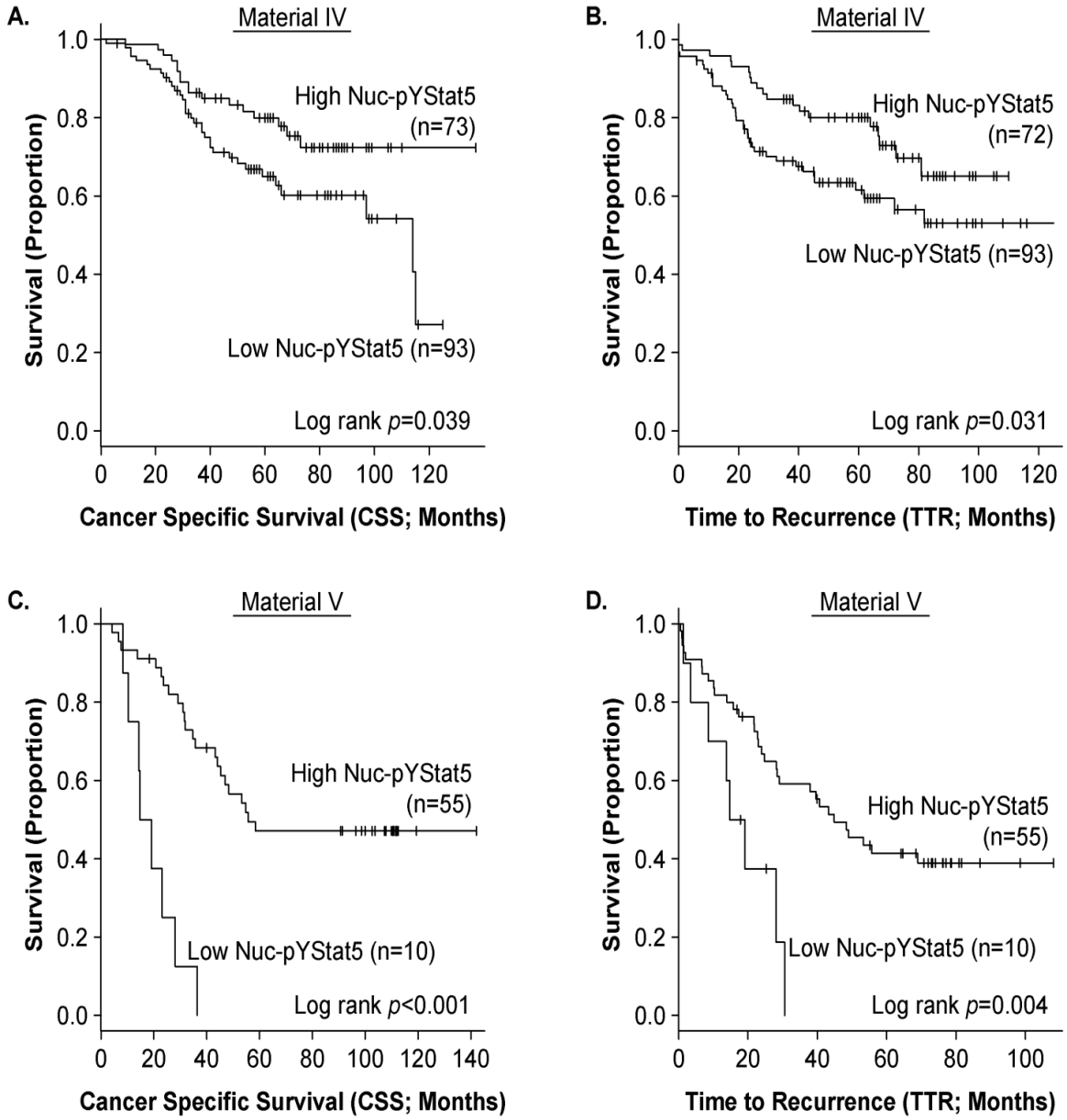

Figure 3 - Low levels of Nuc-pYStat5 predict increased risk of failure of antiestrogen therapy. (A-B) Low levels of Nuc-pYStat5 detected by DAB-chromogen IHC and pathologist scoring in patients treated with antiestrogen therapy (Cohort IV) predicted (A) poor breast cancer-specific survival (CSS) and (B) reduced time to recurrence (TTR) of breast cancer. (C-D) Immunofluorescence and quantitative AQUA analysis of Nuc-pYStat5 expression in breast cancer patients treated with antiestrogen monotherapy (Cohort V) revealed that low expression of Nuc-pYStat5 was predictive of (C) poor cancer-specific survival (CSS) and (D) reduced time to recurrence (TTR) of breast cancer. Kaplan-Meier plots with censored cases (+) and number of patients per group indicated**.**

Research Project 3: Project Title and Purpose

Stat5 and ErbB2 in Prostate Cancer - Organ-confined primary prostate cancer is typically treated by surgery, radiation, hormone therapy, or different combinations of these three treatment modalities, depending on the age and operability of the patient. If prostate cancer has already invaded the neighboring tissues or metastasized to distant sites by the time of the diagnosis, the main treatment options include radiation, hormone therapy and/or chemotherapy (docetaxel) combined with (neo) adjuvant therapies. However, the existing pharmacological therapies for prostate cancer only provide a temporary relief of the symptoms and the cancer growth, while the hormone-refractory form of prostate cancer develops. Moreover, no effective therapies for metastatic prostate cancer currently exist. In this project, the molecular basis of why positive activation status of transcription factor Stat5a/b may provide a biomarker for sensitivity of prostate cancer to ErbB2-inhibitors as a therapy will be examined.

Anticipated Duration of Project

1/1/2009 – 12/31/2012

Project Overview

In this project, the researcher will test the following central hypothesis: Active transcription factor Stat5a/b mediates resistance of prostate cancer to (neo) adjuvant therapies such as ErbB2 inhibition. Preliminary data demonstrates that active Stat5a/b transcriptionally synergizes with wild-type and mutated androgen receptor (AR) in prostate cancer cells, where Stat5a/b increases transcriptional activity of AR. AR, in turn, increases transcriptional activity of Stat5a/b. Second, we show that epidermal growth factor (EGF) activates Stat5a/b in prostate cancer cells, and, importantly, inhibition of ErbB2 protein expression blocks phosphorylation of Stat5a/b. At the completion of this project it is expected to be established whether activation of Stat5a/b would identify those prostate cancers that respond to ErbB2 inhibition by growth suppression, and whether active Stat5a/b combined with phosphorylated ErbB2 provides a better prognostic indicator of poor clinical outcome than active Stat5a/b alone.

Aim 1) Determine whether ErbB2 activates Stat5a/b in a set of human prostate cancer cell lines, and whether ErbB2 inhibition leads to apoptosis of human prostate cancer cells and decreases prostate xenograft tumor growth through inhibition of Stat5a/b.

Aim 2) Determine whether Stat5a/b is the mediator of the synergetic interaction between ErbB2 and AR in prostate cancer cells.

Aim 3) Determine whether active Stat5a/b combined with phosphorylated ErbB2 provides a better prognostic indicator of poor clinical outcome than active Stat5a/b alone.

Principal Investigator

Marja T. Nevalainen, MD, PhD
Associate Professor

Thomas Jefferson University
Kimmel Cancer Center
Bluemle Life Science Bldg Suite 309
233 South 10th Street
Philadelphia, PA 19107

Other Participating Researchers

P. Vogiatzki, PhD – employed by Thomas Jefferson University

Expected Research Outcomes and Benefits

The concept of Stat5a/b as a determinant of therapeutic response of prostate cancer to ErbB2 inhibition is entirely novel. Previous preclinical studies on the role of ErbB2 in the growth of prostate cancer cells have been relatively unsystematic and have yielded conflicting results. The results of clinical trials on ErbB2 inhibitors in prostate cancer have been disappointing. This may be due to clinical trials having focused on advanced prostate cancer only. Second, the trials have not included any selection methods for patients in terms of ErbB2 positivity or activation status of other key growth regulating kinase pathways of prostate cancer. These studies provide the unique opportunity to determine the role of ErbB2 and ErbB2 inhibitors for prostate cancer growth in preclinical models of prostate cancer.

Summary of Research Completed

The *rationale* behind the proposed research is based on the previous findings of Stat5a/b in prostate cancer growth by the researchers, who have previously shown that Stat5a/b is a critical survival factor for Stat5a/b-positive human prostate cancer cell lines in culture and human prostate cancer xenograft tumors in athymic nude mice. Furthermore, the researchers have shown that Stat5a/b is constitutively active in prostate cancer but not in normal prostate epithelium, and that Stat5a/b activation is strongly associated with high histological grade of prostate cancer. Prolactin (Prl) is one of the key activators of Stat5a/b in human prostate cancer, and the applicants have previously demonstrated that Prl is locally produced at high quantities by prostate cancer epithelium. The investigators further showed that Stat5a/b activation in primary prostate cancer predicts early prostate cancer recurrence and demonstrated that active Stat5a/b transcriptionally synergizes with androgen receptor (AR) in prostate cancer cells, where Stat5a/b increases transcriptional activity of wild-type(Wt) AR liganded by dihydrotestosterone (DHT). WtAR, in turn, increases transcriptional activity of Stat5a/b.

In the current reporting period, the investigators generated tissue microarrays of clinical prostate cancers from patients treated by either radical prostatectomy or by watchful waiting. The demographic information of the patients samples was collected (Table1) and the tissue microarrays were immunostained for nuclear Stat5a/b (Fig. 1).

The investigators show that in patients treated by radical prostatectomy, high nuclear Stat5a/b predicted early disease recurrence in both univariate ($p<0.0001$) and multivariate ($HR=0.62$; $p<0.01$) analysis in the entire cohort, and in intermediate Gleason (Gl.) score (6 and 7) patients

by univariate analysis (p<0.0001) and multivariate analysis (HR=0.55; p=0.017) (Fig.2). In addition, high nuclear Stat5a/b predicted early Prostate cancer-specific death after radical prostatectomy in intermediate Gl. score prostate cancers (p=0.028) by univariate analysis (Fig.2).

In the second group of patients treated by watchful waiting, elevated nuclear Stat5a/b expression was associated with early prostate cancer-specific death (p=0.0453) by univariate analysis (60% increased risk of death; p=0.034) (Fig.3). In conclusion, elevated nuclear Stat5a/b was an independent predictor of increased risk of therapy failure in prostate cancers treated by radical prostatectomy including patients with intermediate Gl. Score prostate cancers. High nuclear Stat5a/b expression predicted early prostate cancer-specific death in patients treated by watchful waiting (Fig.3).

The investigators have tested and set up immunostaining conditions for an anti-ErbB2 antibody (Fig.4) after testing three antibodies from different vendors. The next step is to immunostain the tissue microarrays immunostained for nuclear Stat5 using the antibody recognizing ErbB2, score the staining of individual prostate cancers and carry out the statistical survival analyses.

Table 1. Characteristics of the prostate cancers in Materials I and II.

	Material I				**Material II**			
Variables	**Total number of prostate cancers (n=632)**		**Cancers with Stat5a/b expression status (n=562)**		**Total number of prostate cancers (n=419)**		**Cancers with Stat5a/b expression status (n=106)**	
	n	Median (range)	n	Median (range)	n	Median (range)	n	Median (range)
Age at operation, years	632	63 (40-74)	562	63 (40-74)	419	73.6 (51-95)	106	73.9 (51-88.1)
Follow-up time, years	629	7.3 (0.16-24.7)	562	7.3 (0.16-24.7)	419	5.2 (0-25)	106	5.3 (0.1-18.2)
RFS follow-up, years	627	3.7 (0-19.4)	560	3.6 (0.1-19.4)				
Preoperative PSA μg/L	584	8.0 (0.58-290.0)	523	8.2 (0.58-290)				
RFS, follow-up time, years	627	11.4 (8.8,19.4)*	560	9.9 (6.8,-)*				
Tumor size	579	15 (1-100)	521	15 (1-100)				
	n (%)		**n (%)**		**n (%)**		**n (%)**	
Gleason score								
4	14 (2.2)		7 (1.3)		14 (3.3)		1 (0.9)	
5	49 (7.8)		40 (7.1)		84 (20.1)		28 (26.4)	
6	179 (28.3)		159 (28.3)		110 (26.3)		20 (18.9)	
7	252 (39.9)		232 (41.3)		72 (17.2)		16 (15.1)	

8	83 (13.1)	78 (13.9)	50 (11.9)	13 (12.3)
9	32 (5.1)	31 (5.5)	68 (16.2)	24 (22.6)
10	-	-	21 (5.0)	4 (3.7)
unknown	23 (3.6)	15 (2.7)		
Stage				
pT1	5 (0.8)	5 (0.9)	T1a	27 (25.4)
			73 (17.4)	
pT2	327 (51.7)	279 (49.6)	T1b	28 (26.4)
			137 (32.7)	
pT3	276 (43.7)	259 (46.1)	T2	17 (16.0)
			107 (25.5)	
pT4	1 (0.2)	1 (0.2)	T3	29 (27.3)
			81 (19.3)	
			T4	4 (3.9)
			13 (3.1)	
unknown	23 (3.6)	18 (3.2)	unknown	1 (0.9)
			8(1.9)	
Extra-capsular extension				
Yes	252 (39.9)	237 (42.2)		
No	353 (55.9)	303 (53.9)		
Unknown	27 (4.3)	22 (3.9)		
Positive surgical margins				
Yes	240 (38.0)	216 (38.4)		
No	377 (59.7)	337 (60.0)		
Unknown	15 (2.4)	9 (1.6)		
Seminal vesicle invasion				
Yes	84 (13.3)	81 (14.4)		
No	537 (85.0)	474 (84.3)		
Unknown	11 (1.7)	7 (1.3)		
Lymph node involvement				
Yes	30 (4.8)	29 (5.2)		
No	588 (93.0)	522 (92.9)		
Unknown	14 (2.2)	11 (2.0)		
Stat5a/b nuclear staining score				
0	133 (21.0)	133 (23.7)	11 (2.6)	10 (9.4)
1	182 (28.8)	182 (32.4)	26 (6.2)	24 (22.6)
2	196 (31.0)	196 (34.9)	53 (12.7)	51 (48.2)
3	51 (8.1)	51 (9.1)	26 (6.2)	21 (19.8)
Unevaluable	70 (11.1)	-	303 (72.3)	-

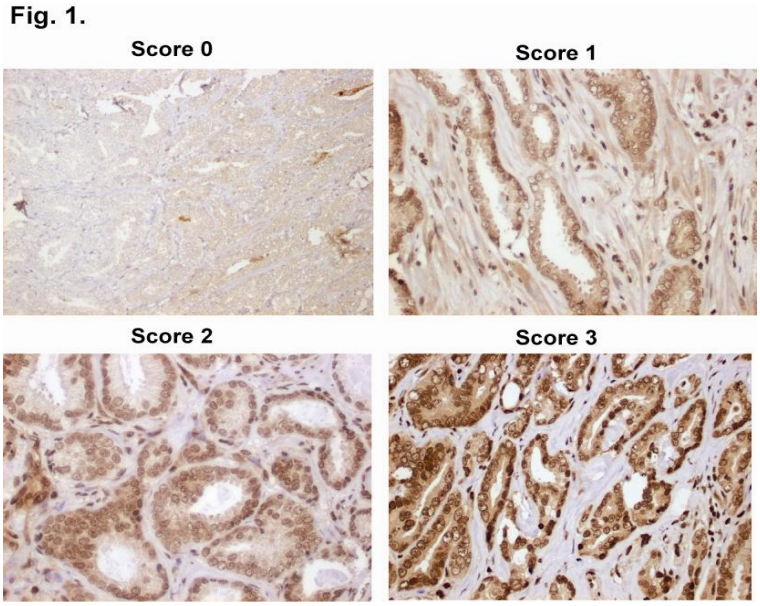

Figure 1. Immunohistochemical detection of Stat5a/b in prostate cancer. Paraffin-embedded sections of prostate cancer tissue microarrays were immunostained with a monoclonal anti-Stat5a/b antibody and biotin-streptavidin amplified peroxidase antiperoxidase immunodetection. 3,3'-Diaminobenzidine was used as chromogen and Mayer's hematoxylin as counterstain. Individual prostate tissue microarray cores in both Material I and II were scored for nuclear Stat5a/b levels on a scale from 0 to 3, where 0 represented negative (*top*), 1 weak (*second from top*), 2 moderate (*second from bottom*) and 3 (*bottom*) strong immunostaining. The final score for each patient was the maximum of the individual core scores.

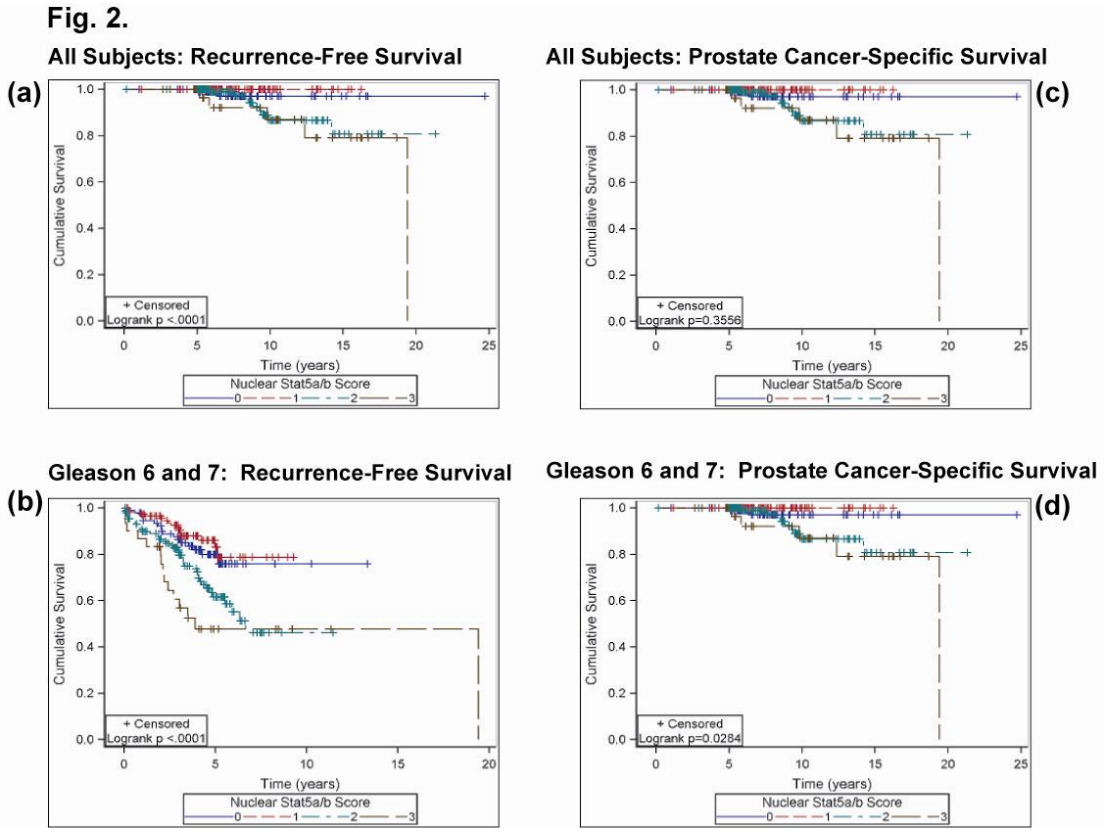

Figure 2. High levels of nuclear Stat5a/b expression predicts early lethal disease recurrence of prostate cancer after radical prostatectomy (Material I). Kaplan-Meier analyses indicating that high nuclear Stat5a/b expression predicts shorter recurrence-free survival in all patients regardless of Gleason (Gl.) scores (n= 560) as well as in intermediate Gl. score prostate cancer patients (n=379) (a and b). In addition, high nuclear Stat5a/b expression in prostate cancer after surgical treatment predicted shorter prostate cancer-specific survival (c and d).

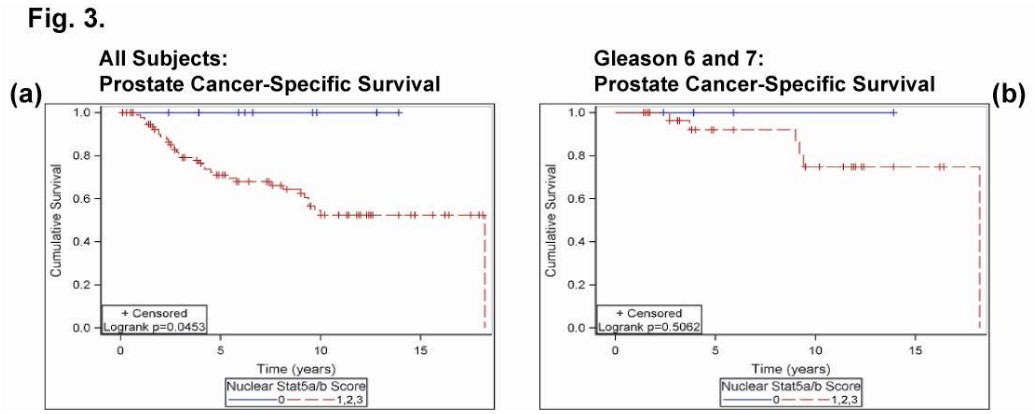

Figure 3. High levels of nuclear Stat5a/b expression in prostate cancer predicts shorter prostate cancer specific-survival in patients treated with watchful waiting (Material II). Kaplan-Meier curves for prostate cancer-specific survival according to negative (top curve) or positive (bottom curve) Stat5a/b activation status in all patients regardless of Gl. score (n=106) (a) and in Gl. score 6 and 7 patients (n=36) (b).

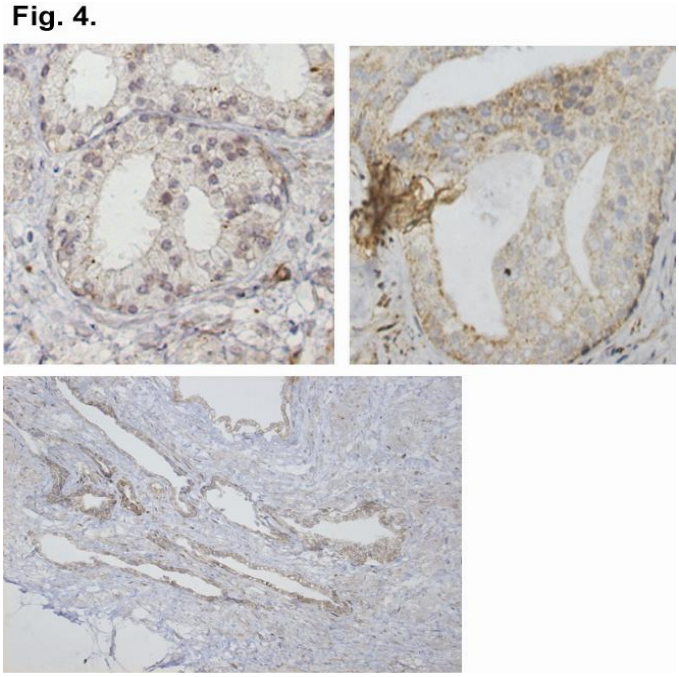

Figure 4. Immunostaining of ErbB2 in clinical prostate cancers. Paraffin-embedded sections of prostate cancer tissue microarrays were immunostained with a monoclonal anti-ErbB2 antibody and biotin-streptavidin amplified peroxidase antiperoxidase immunodetection. 3,3'-Diaminobenzidine was used as chromogen and Mayer's hematoxylin as counterstain.

Research Project 4: Project Title and Purpose

Targeting the IGF-I Receptor in Cancer - This project proposes to determine conditions which will maximize the therapeutic effect of antibodies to the insulin growth factor I (IGF-I) receptor (a receptor for a growth factor) in cancerous tumors. Many cancers (including lung, colon and breast cancers), have already shown susceptibility to this treatment, and these antibodies are currently being used in clinical trials. Clinicians are now anxious to know which human tumors are most sensitive to the antibodies to the IGF-I receptor. There are intra- and extra-cellular factors that condition the response of tumor cells to treatment and the purpose of this project is to identify these conditions.

Anticipated Duration of Project

1/1/2009 - 12/31/2012

Project Overview

Specific Aim # 1: IRS-1 Acetylation and its Effect on IRS-1 Function. This aim focuses on the IGF-1 receptor (IGF-IR) and its docking protein, insulin receptor substrate I (IRS-1), and their role in colon cancer. The hypothesis is that IRS-1 is the key molecule in the role of the IGF-IR

in cancer, and could possibly be a biomarker for sensitivity of colon cancer cells to antibodies to the IGF-IR.

Specific Aim # 2: Role of IRS-1 in oncogenesis and its relationship to the EGFR. A problem that confronts clinicians when using antibodies to growth factor receptors in cancer therapy is the ability to identify tumors that are particularly sensitive to targeting. This project will focus on why certain tumors become resistant to therapy with receptor antibodies. This is well illustrated in antibodies to the epidermal growth factor receptor (EGFR) that are currently used in clinical practice. This aim will study the problem of resistance to therapy in breast and lung cancer cells, based on the hypothesis that IRS-1 plays a major role in resistance. In addition, we will study the role of Stat proteins in cancer in relation to the interaction with IRS-1.

The objectives will be accomplished using mass spectrometry, and molecular and cell biology methodologies with which this laboratory has over 20 years of experience. Levels of IRS-1 can be modulated by down-regulating it or by increasing it through ectopic expression.

Principal Investigator

Renato Baserga, MD
Distinguished Professor
Thomas Jefferson University
Bluemle Life Sciences Bldg.
233 S. 10th Street
Philadelphia, PA 19107

Other Participating Researchers

Andrew Quong, PhD, Gasparre Larroca, PhD - employed by Thomas Jefferson University

Expected Research Outcomes and Benefits

The outcome of this project is to provide new criteria for the treatment of human cancer with antibodies to the IGF-I receptor. The ongoing clinical trials have indicated that antibodies against the IGF-I receptor are effective against various forms of cancer, and Phase II clinical trials are now being carried out at several institutions in cancers of the lung, breast, and colon, brain tumors and bone sarcomas. No cancer treatment is effective against all forms of cancer, and resistance to treatment is unfortunately a frequent outcome with almost all therapies. The benefits of this research will allow clinicians to apply the specific therapy that will yield the best results when using antibodies to the IGF-IR. The project will also define the mechanisms of resistance of cancer cells to therapeutic interventions. This is an exquisitely translational research project, with basic science exploring modalities to be directly applied in clinical venues.

Summary of Research Completed

This project shows the crucial importance of IRS-1 on the growth of colon cancer cells. This project targeted IRS-1 with microRNA 145, which was previously shown to down-regulate IRS-

1 (but not IRS-2), and the IGF-I receptor by binding to the 3'UTR of their mRNAs. miR145 has been proposed as a tumor suppressor. It was found that an IRS-1 lacking its 3'UTR is no longer down-regulated by miR145 and rescues colon cancer cells from miR145-induced inhibition of growth. An IGF-IR resistant to miR145 (again by elimination of its 3'UTR) is not down-regulated by miR145, but fails to rescue colon cancer cells from growth inhibition. These results indicate that down-regulation of IRS-1 plays a significant role in the tumor suppressor activity of miR145. Also found was that all-trans retinoic acid (ATRA) stops the growth of mammary cancer cells, and that the inhibition is tied to the down-regulation of IRS-1 (but, not IRS-2). This suggests that ATRA may act on cell growth through miR145, that also down-regulates IRS-1 but not IRS-2. This hypothesis is now being tested.

These results have been published in three articles in high profile journals. We have also tried to determine (in collaboration with Andrew Quong, Ph.D. of Thomas Jefferson University) the IRS-1 residues acetylated. We have been able to determine that the acetylated residues are in the first 300 amino-acids of IRS-1, but more precise determinations were not conclusive.

Finally, we investigated the relationship of the IGF-IR signaling pathway to DACH1, a tumor suppressor of breast cancer cells. The mammalian homologue of the Drosophila dachshund gene (DACH1) has been reported as a tumor suppressor in human breast and prostate cancers. It down-regulates the epidermal growth factor receptor (EGFR) and cyclin D1. The signaling pathway of the type 1 insulin-like growth factor receptor (IGF-IR) is known to be responsible for the development of resistance to treatment of human cancer with antibodies to the EGFR. We investigated as to whether DACH1 still exerts its tumor suppressor activity in cells dependent on the IGF-IR for growth. The findings were that in cells growing in IGF-1 (and unresponsive to EGF), DACH1 is devoid of tumor suppressor activity.
The Drosophila dachsund (dac) gene is the founding member of the DACH subfamily encoding a nuclear protein essential for the development of Drosophila eye, limb and brain. The DACH1 protein of mammalian cells is decreased in human breast cancer compared to normal mammary gland. Analysis of over 2,000 human breast cancer samples showed an inverse correlation between levels of nuclear DACH1 expression and mitotic index and predicted survival. DACH1 levels are also decreased in prostate cancer and its ectopic expression inhibits prostate cancer cells proliferation in xenotransplants. Over-expression of DACH1 down-regulates both the EGFR and cyclin D1 levels, confirming its role as a growth inhibitor. DACH1 is considered a tumor suppressor.

The implications of these findings, although of a negative nature, are actually of considerable interest. The evidence is clear that nuclear DACH1 is down-regulated in human breast cancers, and its role as a tumor suppressor has been confirmed experimentally in breast and prostate cancers, both of epithelial origin. There is scattering in nuclear DACH1 levels in specimens of human breast cancer, and it is a legitimate question to ask how these cells manage to grow in the presence of normal levels of a tumor suppressor. For a number of years, investigators had noted that development of cancer cells resistance to EGFR targeting involved activation of the IGF-IR (see for instance Chakravarti et al. with many references). Sharma et al. went further and claimed that IGF-IR signaling is responsible for the development of drug-resistance in subpopulations of cancer cells in a more general way, including resistance to antibodies to the EGFR and chemotherapeutic agents.

In addition, a number of observations have shown that cancer cells switch to other growth factors when a growth factor receptor is targeted, for instance with an antibody. It has been known for some time that there is a cross talk between the IGF-IR and EGFR, and since then, numerous reports have appeared showing that the IGF-IR signaling pathway is often responsible for the development of resistance to treatment with antibodies to the EGFR. Since the IGF-IR is often antagonist to EGFR targeting, this project investigated whether in the case of DACH1, the IGF-IR also acted by evading the tumor suppressor activity in those cells with normal DACH1 levels. Our results show that the IGF-IR is independent of DACH1 action and that cells growing in IGF-1 are not subject to inhibition by DACH1.

This project proposed that the IGF-IR may provide the growth factor necessary to evade the tumor suppressor activity of DACH1. In addition, it was proposed that in mammary cancer cells where DACH1 is not down-regulated, or very little, cells may grow because they express substantial amounts of IGF-IR and respond to growth through IGF1. Our prediction is that cancer cells with normal levels of DACH1 will be found to express substantial levels of IGF-IR and/or IRS-1, its docking protein that sends a strong proliferative, anti-differentiation and transformation signal.

These studies have been summarized in a Cell Cycle 10:12, 1956-1959; June 15, 2011; © 2011 Landes Bioscience.

Research Project 5: Project Title and Purpose

The Role of MicroRNA (miRNA) Gene Expression in Therapy Resistance of Human Breast Cancer - This year breast cancer will kill over 40,000 women in the United States, and there will be over 210,000 new cases, according to statistics from the American Cancer Society and Centers for Disease Control. Since the risk of developing breast cancer increases with age, the prevalence of this disease can be expected to increase as the overall population continues to age. However, studies on the underlying genesis and progression of breast cancer, utilizing the latest techniques of molecular biology, offer hope of finding more effective treatments. Studies over the last two years have demonstrated that the presence of "stem cells" which are found within human breast cancer, contribute to therapy resistance. This project will focus on a class of genes called the miRNA found in breast cancer stem cells, and their role in therapy resistance and breast cancer metastasis.

Anticipated Duration of Project

1/1/2009 - 12/31/2012

Project Overview

The long term goal of this project is to obtain important information about the molecular events associated with breast cancer, and develop new molecular targets with which to improve the treatment. Metastatic breast cancer is incurable and lethal: its treatment at present is only palliative, intended to relieve pain and suffering, but not to cure the disease. In order to understand metastatic breast cancer this project will identify new molecular targets for its

treatment, by isolating cells involved in the progression from the primary tumor to the metastatic tumor, and determine the changes in miRNA gene expression that accompany this progression.

The specific aims and methods of the project are:
1) Isolate the cellular intermediates in the progression from the primary breast tumor to the metastatic tumor and determine the changes in miRNA gene expression that accompany this progression. Based upon evidence that circulating tumor cells (CTCs) found in the peripheral blood are linked to the spread of breast cancer, a combined screening called the CellSearch system will be used to identify CTCs from patients with metastatic disease.
2) Elucidate the changes in miRNA expression in breast cancer associated with the development of resistance to tamoxifen and chemotherapeutic agents therapy. The miRNA expression profiles in tamoxifen-resistant tumors and cell lines selected in culture will be determined. These will be compared to the miRNA expression profiles in their tamoxifen-sensitive counterparts as either tumors or the parental cell lines in culture.
3) Elucidate the miRNA signatures regulating breast cancer stem cells. The migration of these mammary stem cells in response to stem cell factor (SCF) will be examined. To determine the specificity of the cells enriched by epitope markers in SCF, complementary approaches will be used: 1. slide populations (SP) analysis; 2. epitope staining for Sca1 and other putative progenitor cell markers; 3. BrdU labeling retention; and 4. heterotypic transplantation.

Principal Investigator

Richard G. Pestell, MD, PhD
Director, Kimmel Cancer Center
Thomas Jefferson University
233 S. 10th Street, 1050 BLSB
Philadelphia, PA 19107

Other Participating Researchers

Mathew Casimiro, PhD, Kongming Wu, PhD, Sanjay Katiyar, PhD - employed by Thomas Jefferson University

Expected Research Outcomes and Benefits

One of the keys for improving current modes of cancer treatment is identifying which specific genes are being expressed in tumors. Using this approach could lead to the development of treatments tailored to the unique gene expression patterns in breast cancer patients. This study will focus on the patterns of miRNA expression in relation to the interplay of cellular factors affecting the growth of breast cancer cells, on the changes in miRNA expression associated with the most lethal stage of breast cancer, namely metastasis, and on the changes in miRNA expression that are associated with resistance to chemotherapy.

Historically, it has been both time-consuming and technically difficult to screen large numbers of tumors for cancer-specific gene expression. To overcome these problems, a powerful tool for the study of gene expression called microarray analysis was employed. Essentially, a custom

"biochip" that combines tens of thousands of gene probes on a single glass slide was created by researchers here at the Kimmel Cancer Center. It has enabled efficient screening for the expression of thousands and thousands of genes in a broad range of human tumors (referred to below as "expression profiling"). Knowing which of the hundreds of miRNA genes are preferentially expressed in various cancers could help to improve diagnosis and lead to innovative therapies for those cancers.

Summary of Research Completed

Aim 3 Results

Cyclin D1 activates STAT-JAK signaling. In order to examine the gene expression profile regulated by endogenous cyclin D1 and endogenous Rb, genome wide expression analysis was conducted. DAVID analysis identified functional pathways regulated by cyclin D1 and Rb including cytokine and chemokine signaling and JAK-STAT signaling. Our previous studies had demonstrated that cyclin D1-induced STAT-dependent gene expression. Cyclin D1 induced γ-interferon-dependent signaling using a multiple synthetic γ-interferon-activated sequences (GAS) response element γ-interferon-activated sequences (GAS_8LUC). In view of the gene expression profiles reflecting reduced STAT signaling in *cyclin D1*$^{-/-}$ MEFS, further analysis was conducted of *cyclin D1*$^{-/-}$ vs wild type MEFs.

In order to examine the role of endogenous cyclin D1 on STAT signaling, Western blot was conducted using exponentially growing fibroblasts. Growth hormone activated STAT-5 phosphorylation (Figure 1A). Growth hormone induced STAT-5 phosphorylation either in exponentially grown or confluent-starved cells (Figure 2A). Similarly, in *cyclin D1*$^{-/-}$ cells, growth hormone failed to activate STAT-5 phosphorylation. Similar observations were made for both STAT-5b (Figure 1B). The requirement for cyclin D1 in activation of STAT-5 signaling was examined further. Prolactin induced STAT signaling within 4 minutes of treatment (Figure 1C). However, *cyclin D1*$^{-/-}$ cells failed to show any induction of STAT-5a/b phosphorylation. STAT-5a and b are activated by JAK-2 phosphorylation. STAT-5b mediates promoted biological effects of growth hormone whereas STAT-5a transmits predominantly signals transmitted by the prolactin receptor.

However, STAT-5a and b are activated by several different ligands including IL-2, IL-3, IL-5, IL-7, GCSF, insulin and others. The addition of growth hormone induced tyrosine phosphorylation of JAK-2. However, the induction was reduced in *cyclin D1*$^{-/-}$ cells, both in exponentially growing and in confluent starved cells (Figure 1D). Reintroduction of cyclin D1 into *cyclin D1*$^{-/-}$ cells was sufficient to restore tyrosine phosphorylation of STAT-5a/b (Figure 1F). JAK-STAT signaling is negatively regulated by Suppressors Of Cytokine Signaling (SOCS molecules). SOCS negatively regulates JAK-STAT signaling by binding to cytokine receptors and the activation loop of JAK through their central SH2 domain. A short kinase inhibitory domain in SOCS1 and SOCS3 also interacts with JAK.

Recent studies have demonstrated that SOCS and STAT signaling are under control of miRNA regulatory loops. We therefore interrogated miRNA of the *cyclin D1*$^{-/-}$, *Rb*$^{-/-}$, and *cyclin*

D1$^{-/-}$/Rb$^{-/-}$ MEFs. miRNA differentially expressed in the *cyclin D1$^{-/-}$* cells compared with wild type including mIR-221/222, mIR-155, and Let-7a (Figure 2A). Twenty miRNA were selectively altered in abundance in the *cyclin D1$^{-/-}$*, six miRNA were selectively altered in the *pRb$^{-/-}$*, and thirteen miRNA were lost in both *cyclin D1$^{-/-}$ and Rb$^{-/-}$* cells (Figure 2A). miR-16B and 24 were reduced in *cyclin D1$^{-/-}$* cells (Figure 2A). Northern Blot analysis confirmed miR-16 was unaltered in the *pRB$^{-/-}$* but reduced in the *cyclin D1$^{-/-}$* and re-expression of cyclin D1 in *cyclin D1$^{-/-}$* MEFs restored miR-16 abundance. miR-24 abundance was reduced in the *cyclin D1$^{-/-}$* cells (Figure 2B). The *pRb$^{-/-}$* cells showed a reduction in miR-221 (Figure 2A). Re-expression of pRb induced miR-221 (data not shown). Cyclin D1a expression did not affect miR-221 consistent with the original micro RNA analysis. An analysis of miRNA enriched in breast cancer stem cells (Figure 2B), demonstrated an overlap (in yellow) with miRNA regulated by either cyclin D1 or pRB.

<u>Cyclin D1 mediates heterotypic signals that promote stem cell expansion.</u> In view of the finding of decreased STAT activity in *cyclin D1$^{-/-}$* cells, we considered the possibility that cyclin D1 may promote cytokine signaling. *Cyclin D1$^{-/-}$* mice demonstrate failed terminal alveolar breast bud development which has been attributed to a failed expansion of a progenitor cell pool. In order to determine whether cyclin D1 mediates heterotypic signals that promote stem cell expansion a surrogate assay was conducted using mouse embryonic stem (mES) cells in a co incubation experiment. Co incubation of ES cells with media from either wild type, *pRB$^{-/-}$, cyclin D1$^{-/-}$, or pRB/cyclin D1$^{-/-}$* cells demonstrated a reduction in the relative number of ES cells upon deletion of either *cyclin D1* or *pRb*.

In view of our finding that cyclin D1 promoted ES cell expansion via heterotypic signals, and recent findings demonstrating cyclin D1 plays a role in expansion of mammary progenitor cells that are targets of MMTV-ErbB2, we examined the possibility that cyclin D1 may contribute to breast tumor initiating cells (BTIC) via heterotypic signals *in vivo*. As a form of positive control we examined the relative distribution of $CD24^+/CD29^+/Lin^-$ cells in the mammary gland of virgin mice. Consistent with recent publications, the relative proportion of progenitor cells was not decreased in the *cyclin D1$^{-/-}$* mice (Figure 3 A,B). In contrast, the mammary stem cell population of pregnant mice showed a significant reduction in the relative proportion of $CD29^+/Lin^-$ cells in the *cyclin D1$^{-/-}$* mammary gland. These findings are consistent with recent observations that the proportion of SCA-positive cells are reduced in the *cyclin D1$^{-/-}$/cyclin D1^{KE}* knockin double transgenic mice.

Collectively these preliminary studies identify the molecular signature of miRNA regulated by cyclin D1 and suggest a role for cyclin D1 in regulating stem cell expansion via a heterotypic signal. The ongoing studies will determine the miRNA circuitry regulating the heterotypic signal governing stem cell expansion.

Figure 1

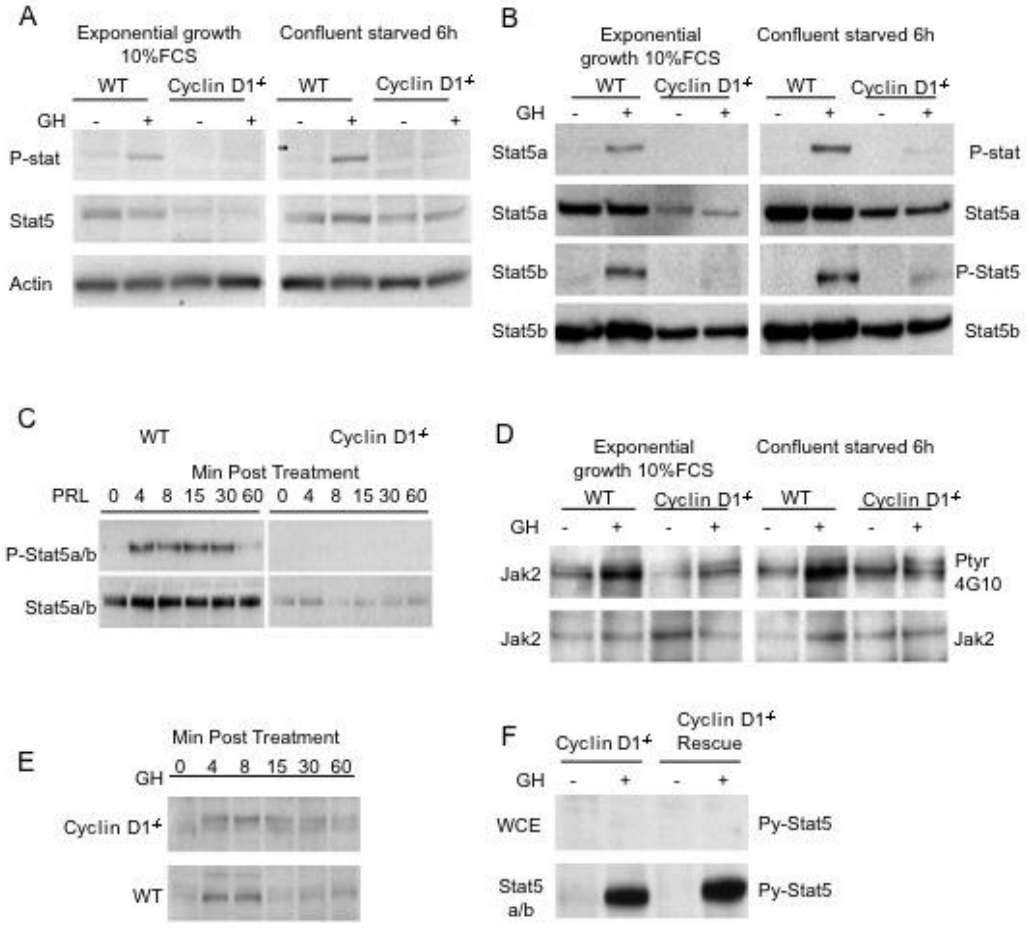

Figure 1. Cyclin D1 regulation of STAT activity. (A) Western blot of MEFs (wildtype vs. cyclin D1$^{-/-}$) either exponentially growing or confluent. Cells were treated with growth hormone. Antibodies are directed to thorycine phosphorylated STAT 5 or b actin as indicated. (B) Western blot conducted with antibodies as indicated (C) Prolactin treatment of MEFs for the time points indicated (D,F) cyclin D1 wildtype or cyclin D1$^{-/-}$ MEFs treated with growth hormone for the time points indicated were subjected to Western blot with the antibodies as indicated.

Figure 2

A

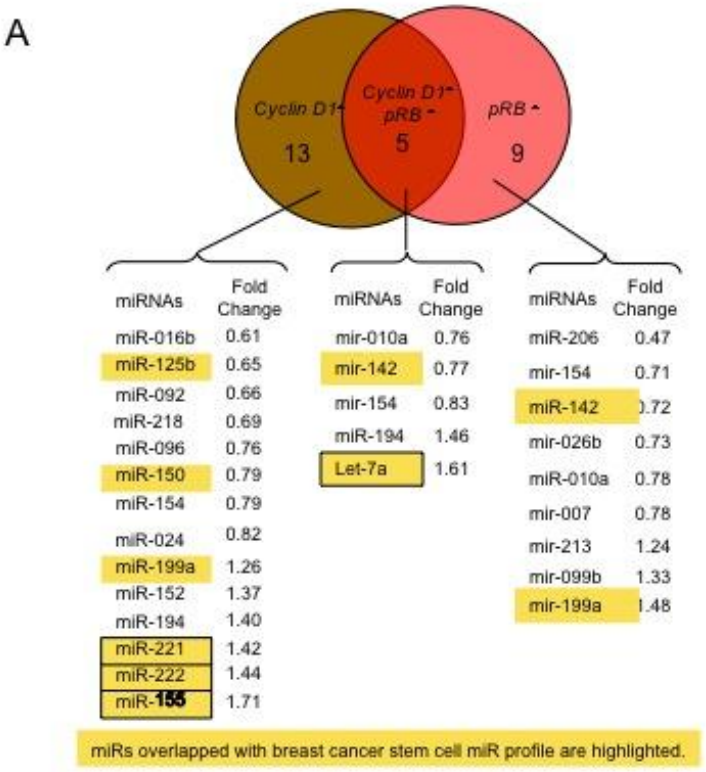

B

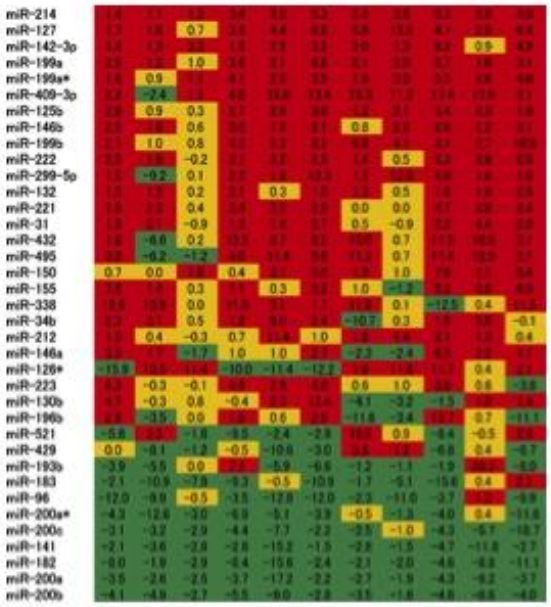

Figure 2. Cyclin D1 vs. pRB micro RNA expression profiling. Micro RNAs derive from cyclin D1$^{-/-}$, pRB$^{-/-}$ or cyclin D1^{-}, pRb$^{-/-}$. MEFs were compared and are shown within the Venn Diagram. (B) In yellow are micro RNAs shown previously to play a role in regulating stem cell function.

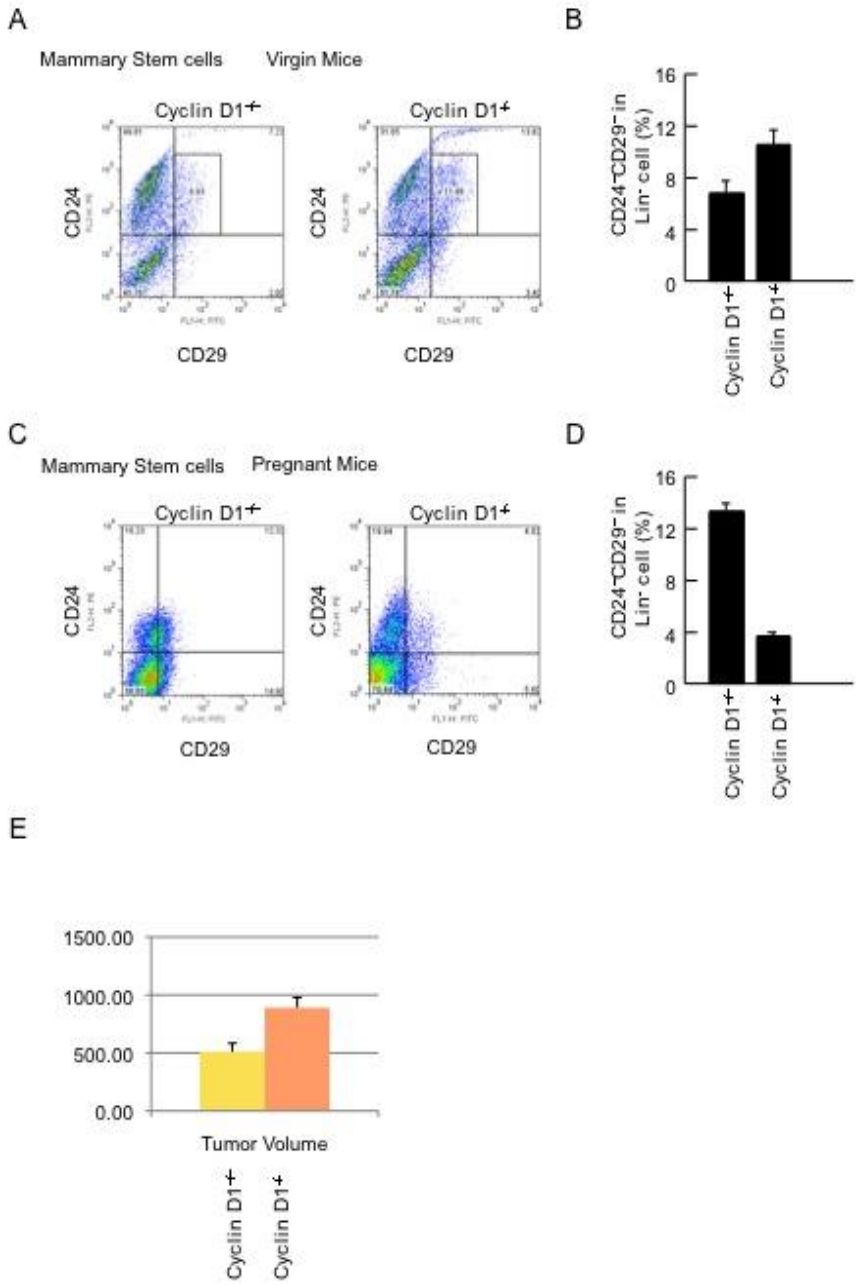

Figure 3. Cyclin D1 expands mammary stem cell population. FACS based cell sorting for mammary epithelial stem cells using the CD24/CD29-lin- cells in either virgin (wt vs *cyclin D1*$^{-/-}$,) mice or (C,D) pregnant mice mammary glands.

Research Project 6: Project Title and Purpose

Mechanisms for Metastasis Suppression through Kisspeptin Regulation of the Microenvironment - Metastasis (spreading) is an unfavorable milestone in the clinical course of cancer. The ability of tumor cells to spread from the primary site and invade normal tissues requires a specific set of properties enabling them to proliferate and migrate. It is also critical that these malignant cells have a supportive niche within which they can expand. The KiSS1 gene was discovered based on its ability to block metastasis of human cells in mouse models of melanoma. Current evidence suggests that the product of this gene is secreted by tumor cells and prevents the migrating cells from developing a niche. These experiments, which will elucidate the mechanisms of action, may provide novel, non-toxic approaches for the treatment and prevention of tumor metastasis.

Anticipated Duration of Project

1/1/2009 - 12/31/2012

Project Overview

Metastasis is a grim milestone in the majority of cancers. The spread of tumor cells to secondary sites requires a cascade of properties that enable them to invade normal tissues, migrate into blood vessels, and proliferate while detached from other cells. Also required is a receptive, supportive environment that can be induced by the tumor cells through tissue remodeling, and stromal cells to provide a microenvironment that fosters growth. The cellular elements of this microenvironment include inflammatory cells, endothelial cells, fibroblasts, and myofibroblasts. The latter two populations have been designated carcinoma-associated fibroblasts, and these cells have been found to promote malignant properties. The stroma of metastatic tumors have highly similar gene expression patterns to that of wound healing, and is therefore associated with the "wound-response gene signature" of metastasis and poor prognosis.

The KiSS1 gene encodes a secreted protein that is processed to peptides (kisspeptins: KP). KP was discovered to be absent from metastatic tumors, and able to suppress metastasis in model systems. While KPs are ligands for GPR54, a G protein coupled receptor, the mechanism for metastasis suppression has not been elucidated, and the cells that express GPR54 have not been identified. Since KP expression can inhibit pulmonary metastasis from tumor cells that lack GPR54 expression, it is likely that a paracrine mechanism is active. It has been demonstrated that low levels of GPR54 are expressed by fibroblast cell lines. The objective of this project is to elucidate the paracrine mechanism responsible for metastasis suppression by kisspeptins, and to identify GPR54+ target cells responsible for these effects. The hypothesis of the project is that KP secretion decreases the formation of activated stromal fibroblasts and myofibroblasts. This hypothesis will be tested in mouse wound healing (Specific Aim 1) and pulmonary fibrosis (Specific Aim 2) models to determine whether administration of KPs or novel downsized analogs, can block the formation of the fibroblastic microenvironment.

Principal Investigator

Stephen C. Peiper, MD
Peter A. Herbut Professor and Chair
Thomas Jefferson University
Jefferson Medical College
1020 Locust Street, 279 JAH
Philadelphia, PA 19107

Other Participating Researchers

Jean-Marc Navenot, PhD - employed by Thomas Jefferson University

Expected Research Outcomes and Benefits

Despite advances in chemotherapy, the metastatic spread of cancer is still associated with a poor prognosis, and few effective treatments are available. Kisspeptins (KPs) are ligands (bonding agents) for a G protein coupled receptor, which is the class of targets for about one-third of drugs. Thus, the demonstration that KPs are effective anti-metastatic agents will open the door to a new type of therapy. Prior to the pursuit of a therapeutic role for KPs, it is critical to develop an understanding of the precise mechanisms for suppression of metastasis, which to date has been elusive. The available data indicates that KPs do not directly inhibit the spread of tumor cells. Instead, there is evidence that they control the local environment for migrating tumor cells and prohibit the formation of a supportive niche. Thus, it is possible that a therapy based on KPs would block the ability of tumor cells to establish a receptive environment.

One approach to determining the mechanism for metastasis suppression by KPs, is to study a similar environment and identify its targets that express the corresponding receptor (GPR54). Since there is evidence that GPR54 is expressed in higher levels by lung fibroblasts, we will characterize the effects of KPs to identify relevant targets and mechanisms in pulmonary fibrosis models and in wound healing using mice. This project will also provide insight into the effects of KPs on regenerative processes while maintaining relevance to tumor therapy, because the wound healing environment has extensive molecular similarity to that of malignant tumors. The targeting of drugs to block host responses instead of tumor functions has the potential advantages of decreased toxicity and decreased emergence of resistant tumor cells.

Summary of Research Completed

The objective of this project is to investigate the hypothesis that the anti-metastatic effect of the metastasis suppressor KISS1 is mediated through inhibition of the tissue remodeling that needs to occur in distant organs in order for metastatic cells to proliferate. However, studying the microenvironment around micrometastatic lesions is complicated by the difficulty to identify and locate these lesions in tissues. This tissue remodeling is believed to share some similarities with wound healing and lung fibrosis. The proposed specified aims of this project are to use wound healing and lung fibrosis as experimental models of tissue remodeling around metastatic tumor cells.

The first specific aim focused on skin wound healing in mice. The effect of KISS1 on the tissue repair process was evaluated both at the macroscopic level and microscopic level. The healing of excisional wounds created with a 6 mm dermal biopsy punch was studied during treatment of the animals with local daily injections of kisspeptin 10 (KP10), the biologically active form of KISS1 or FTM145, a synthetic compound that mimics the activity of KP10 but with dramatically improved in vivo stability. In the previous 2 years of the project, we showed that treatment of the mice with KP10 or FTM145 had little effect (if any) on the kinetics of wound healing or on the microscopic tissue organization.

The central hypothesis of this project (the paracrine mechanism of action of KISS1) was based on observations made using the C8161.9 human melanoma xenograft. The human C8161.9 cell line was used by Dr. Danny Welch and colleagues for the original description of the anti-metastatic activity of KISS1. We collaborated with Dr. Welch for some in vitro studies while his group performed the animal studies. We later used the same C8161.9 xenograft model to investigate the capacity of FTM145 to inhibit the metastatic growth of C8161.9 cells into the lungs of nude mice after injection of the tumor cells into the bloodstream. Dr. Welch provided us with the same cells his group has previously used: parental C8161.9 cells, C8161.9 cells transfected with an empty plasmid and expressing EGFP (C8161.9-pc3) and C8161.9 cells transfected with a plasmid coding for a version of KISS1 containing an internal FLAG epitope (KFM) and also expressing EGFP (C8161.9-KFM). To obtain expression of KFM (which is a secreted protein), single cell cloning was necessary. The experiments performed in Dr. Welch's laboratory indicated that both C8161.9-pc3 and C8161.9-KFM were capable of forming orthotopic (intradermal) tumors with similar efficiency. However, whereas C8161.9-pc3 cells could also grow in distant organs (lungs, bones, eyes and kidneys), C8161.9 could colonize these organs but did not form metastatic lesions, remaining instead dormant for extended periods of time. These observations were the foundation for the central hypothesis of this project. In parallel to the wound healing experiments, we also used this model to test a pharmacologic approach to KISS1 anti-metastatic activity, i.e. test whether replacing the secretion of KISS1 by tumor cells by injections of the highly active derived compound FTM145 could also suppress the metastatic growth of C8161.9 cells.

A survival experiment was designed in which C8161.9-pc3 cells were injected into nude mice (tail vein injection) and the mice were treated daily with subcutaneous injections of FTM145 or PBS as a control. As shown in Figure 1, FTM145 offered no survival benefits over PBS despite being fully active. Although administration of a compound may not be as effective as the local secretion of KISS1/KFM, we expected at least a partial inhibition. This led us to reconsider the validity of the C8161.9 xenograft model.

We first characterized the different C8161.9 cells in vitro and found that C8161.9-KFM cells were larger than both the parental C8161.9 cells and C8161.9-pc3 cells. We also found that, whereas C8161.9-KFM could make large numbers of colonies in soft agar, C8161.9-pc3 cells could not and the parental cells could only make a few colonies. However, when 7 colonies (each originating most likely from a single cell) formed by the parental cells were picked and amplified in vitro, all the cells in each clone had uniformly the same morphology as C8161.9-KFM cells. Moreover, these soft agar clones all exhibited an increased capacity to grow colonies in soft agar. These data suggested that the cloning process used to obtain the KFM cells selected a

subpopulation of cells that represents a minority of the original population of cell and that this subpopulation is phenotypically different from the parental cell line, especially in its capacity to grow as single cells.

Five of these soft agar clones (AC2, 3, 4, 5 and 7) were further characterized in vivo. First, we found that, contrary to the published data, C8161.9-KFM cells not only had a decreased metastatic potential but also had decreased capacity to establish orthotopic tumors compared to C8161.9-pc3 cells (Figure 2A). When injected in the tail vein, C8161.9-pc3 cells migrated to the lungs and developed multiple lesions that were clearly visible on the lung surface and largely invaded normal lung tissues as seen in sections (Figure 2B andC)). In comparison, the KFM cells and the AC clones only developed a few small cell clusters. Importantly, the loss of metastatic potential by the soft agar clones was not due to the expression of endogenous KISS1 as indicated by real-time RT-PCR of KISS1 (Figure 2D). In conclusion, the soft agar clones could recapitulate the in vitro and in vivo properties of C8161.9-KFM cells without expressing KISS1. These data further suggested that the loss of metastatic potential of C8161.9 resulted from an artifact of clonal selection rather than from the expression of KISS1.

This fact was demonstrated by obtaining new clones of C8161.9 cells expressing KISS1. Parental C8161.9 cells or C8161.9-pc3 cells were transfected with the plasmid pcDNA3.1-KFM, selected in antibiotics and cloned. Single cell cloning by limiting dilution (as performed in the case of the C8161.9-KFM cells previously used) resulted in only 3 clones (out of over 600 wells) that consisted of large cells similar to the KFM cells. To avoid this cloning bias, transfected cells were seeded alongside untransfected cells that were used as feeders. Limiting dilution was done so that each transfected cell would be plated in antibiotic-free medium with 1,000 untransfected cells with which they could establish supportive contacts. After 5 days, the cells had expended enough and the selection antibiotic was re-introduced. The untransfected cells were killed within 48 hours and the surviving colonies of transfectants were left to expand. After in vitro expansion, the new C8161.9 clones (over 125) were tested for expression of KFM by flow cytometry and ELISA (Figure 3A and B). A total of 17 clones with high and homogenous expression of KFM were selected and tested in vivo, either as single clones or as pools. Most of the clones were made of small cells identical to the majority of the cells in the parental cell line and a few clones consisted of large cells similar to the previous KFM cells. When injected into the tail vein of nude mice, clones made of larger cells (such as clone 2E8) had low metastastatic potential (Figure 3C). Clones made of small cells (such as clone 6F10) extensively invaded the lungs 4 weeks after injection, similarly to C8161.9-pc3 cells. Only one clone of small cells (4F12) exhibited a decreased metastatic potential, although not to the same extent as the previous C8161.9-KFM.

These data demonstrated that the parental C8161.9 cell line was a mixture of cells with diverse phenotypes and a large range of tumorigenic and metastatic potentials. Single cell cloning using regular limiting dilution protocol is heavily biased toward the selection of cells with good capacity to grow as single cells in vitro but strongly reduced tumorigenic and metastatic potentials. When KFM-expressing clones were obtained without this selection bias, they exhibited metastatic potentials that were not related to KFM expression. These data indicate that the C8161.9 model cannot be used to support the hypothesis of a paracrine mechanism of action

of KISS1. They even strongly suggest that KISS1 does not have any significant activity in this xenograft model.

Figure 1

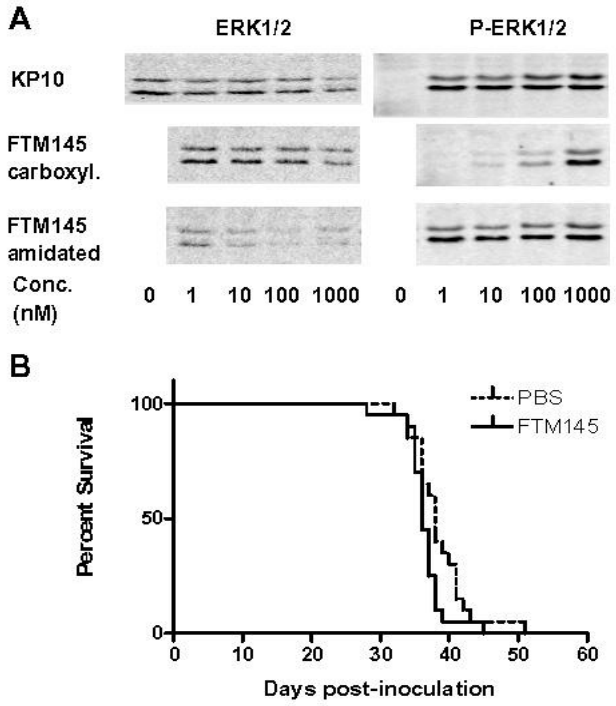

Figure 1: Injection of a KISS1 mimetic does not inhibit metastasis of C8161.9 cells in xenograft experiments. A. KP10 and C-ter-amidated FTM145 activated GPR54 in HEK-293 transfectants with similar potency as demonstrated by phosphorylation of ERK1/2. B. Daily subcutaneous injections of FTM145 did not suppress metastasis in nude mice inoculated with C8161.9 cells and did not offer any survival benefit compared to PBS as shown by Kaplan-Meier analysis.

Figure 2

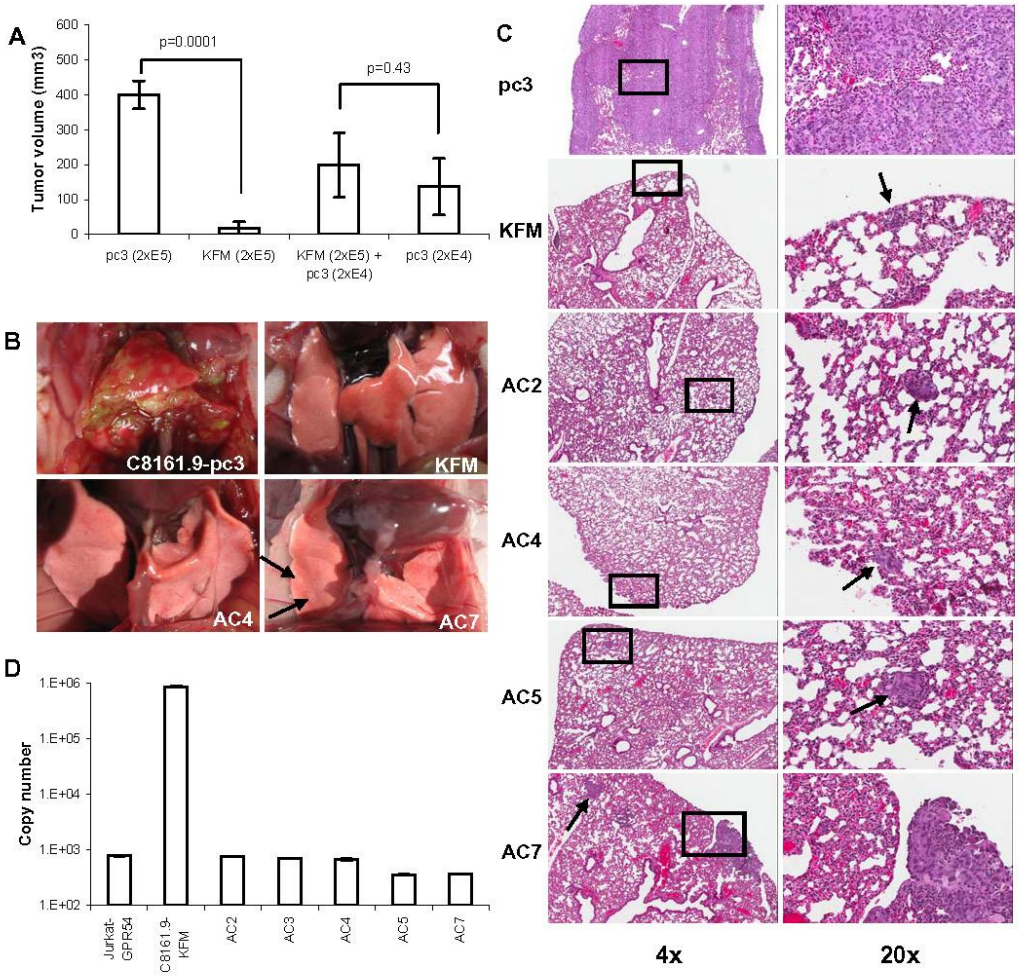

Figure 2: C8161.9 soft agar clones replicated the *in vivo* phenotype of C8161.9-KFM cells without KISS1 expression. A. C8161.9-KFM cells exhibited a strongly reduced capacity to form orthotopic (intradermal) tumors in nude mice and did not suppress the growth of co-injected C8161.9-pc3 cells. Tumors were measured 4 weeks post-injection. Indicated P values were calculated using Student's *t*-test with a 95% confidence interval. B and C. AC clones showed a reduced capacity to form lung metastases similar to C8161.9-KFM cells. Mice were injected in the tail vein with C8161.9-pc3, C8161.9-KFM, AC2, AC3, AC4, AC5 or AC7 cells. After 5 weeks, lungs showed extensive metastasis in mice inoculated with pc3 cells but no or very few (arrows) visible metastatic lesions in mice inoculated with KFM or AC cells. (B) Images are from one representative mouse out of 4 for each clone. Sections of the lungs confirmed that both the number and the size of metastatic lesions (small lesions indicated by arrows) were strongly reduced with KFM or AC cells compared to pc3 cells. Boxed regions of the low-magnification pictures are shown in the right panel. Representative fields out of 4 slides for 4 identical mice for each clone. D. Inhibition of the metastasis potential of AC cells is not related to endogenous KISS1 expression as demonstrated by the absence of detection of KISS1 transcripts by qPCR.

Figure 3

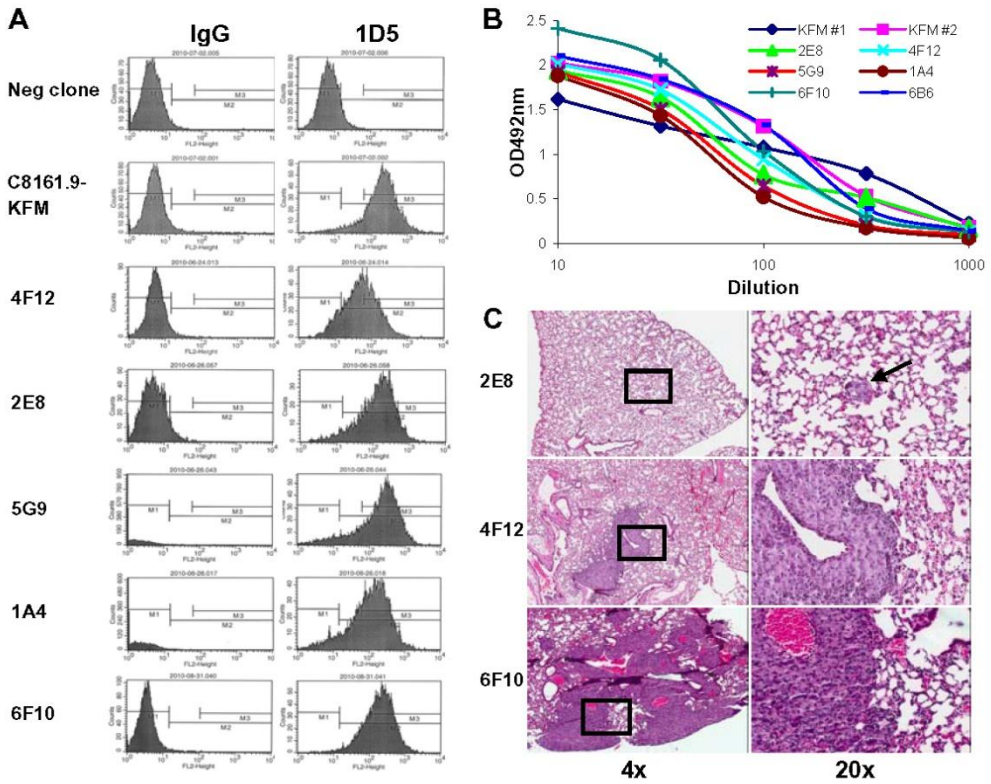

Figure 3: Metastatic potential of new C8161.9 clones is independent from KISS1 expression. New clones of C8161.9 cells expressing KFM displayed a wide range of metastatic potential related to cell morphology but independent of KFM expression. Multiple new C8161.9 single cell clones were derived after transfection with pcDNA3.1-KFM and limiting dilution using non-transfected feeder cells. A. These new clones were tested by flow cytometry for expression of intracellular KFM using a mAb specific for KISS1 (1D5). The histograms show for each clone a single population with a staining intensity similar to the previously described C8161.9-KFM cells. B. Semi-quantitative ELISA for KFM secretion was performed on conditioned media obtained with new KFM clones (shown: clones 2E8, 4F12, 5G9, 1A4, 6F10 and 6B6) in comparison to 2 conditioned media obtained with the original C8161.9-KFM clone previously described. Results showed similar levels of secretion of KFM for the different clones. C. Representative sections of lungs from mice inoculated in the tail vein with new KFM clones and collected after 5 weeks. Clones consisting of large cells similar to KFM cells (e.g. 2E8) had strongly reduced metastasis whereas clones consisting of smaller cells similar to pc3 cells (e.g. 6F10) maintained a metastatic potential similar to C8161.9-pc3 cells. Clone 4F12 had intermediate metastatic potential with fewer but large metastatic lesions. Boxed regions of the low-magnification pictures are shown in the right panel.